




Cite this: *Nanoscale*, 2022, **14**, 2943

# Phase-shift nanodroplets as an emerging sonoresponsive nanomaterial for imaging and drug delivery applications

Weiqi Zhang,  Yuhong Shi, Shazwan Abd Shukor, Aaran Vijayakumaran, Stavros Vlatakis,  Michael Wright and Maya Thanou \*

Nanodroplets – emerging phase-changing sonoresponsive materials – have attracted substantial attention in biomedical applications for both tumour imaging and therapeutic purposes due to their unique response to ultrasound. As ultrasound is applied at different frequencies and powers, nanodroplets have been shown to cavitate by the process of acoustic droplet vapourisation (ADV), causing the development of mechanical forces which promote sonoporation through cellular membranes. This allows drugs to be delivered efficiently into deeper tissues where tumours are located. Recent reviews on nanodroplets are mostly focused on the mechanism of cavitation and their applications in biomedical fields. However, the chemistry of the nanodroplet components has not been discussed or reviewed yet. In this review, the commonly used materials and preparation methods of nanodroplets are summarised. More importantly, this review provides examples of variable chemistry components in nanodroplets which link them to their efficiency as ultrasound-multimodal imaging agents to image and monitor drug delivery. Finally, the drawbacks of current research, future development, and future direction of nanodroplets are discussed.

Received 30th November 2021.

Accepted 19th January 2022

DOI: 10.1039/d1nr07882h

rsc.li/nanoscale

## 1. Introduction

During the last few years, ultrasound technologies have evolved in biomedical applications through imaging and therapeutic areas. These technologies are non-invasive and free of ionising radiation, and can be operated as theranostics. Ultrasound is used in both preclinical and clinical research for anatomical imaging, as well as exerting mechanical forces that lead to either the increase of temperature or cavitation that results in changes in cell membranes while allowing penetration into deep tissue regions. The recent combination of MRI and high intensity focused ultrasound (HIFU) has led to specific site cell ablation in tumour tissues from numerous studies.<sup>1</sup> However, reports of toxicities related to high temperature exposures have hindered the clinical transition. HIFU can induce local hyperthermia that can help drugs to reach tumour regions.<sup>2</sup> However, remarkably, amplified by ultrasound contrast agents (UCAs), also known as microbubbles and recently phase change nanodroplets (PCNDs), ultrasound-mediated drug delivery through cavitation has drawn substantial attention for clinical applications, where physiological and

structural tissue barriers significantly limit the delivery of therapeutic agents to disease sites.

Ultrasound has been a valuable tool for diagnostic and therapeutic applications for more than 60 years.<sup>3</sup> As a mechanical wave, ultrasound will generate cycles of alternating acoustic pressure when it propagates through body tissues and leads to the change of pressure *in situ*.<sup>4</sup> In order to meet clinical requirements, ultrasound contrast agents (UCAs) were developed to enhance ultrasound signals and diagnostics. UCAs possess great clinical values, as they can produce various distinctive imaging and drug delivery characteristics. UCAs can oscillate under ultrasound with low amplitude and produce an acoustic signal, whereas strong oscillation creates shear forces that may lead to poration of nearby cell membranes, *i.e.*, sonoporation. Apart from diagnostics, ultrasound also shows promising potential in therapeutic applications, *e.g.* sonodynamic treatment (SDT). SDT requires two essential components: ultrasound and sonosensitiser molecules. The mechanism of SDT will be introduced later in this review. Sonosensitising nanoparticles could act as cavitation nuclei, including liposomes, micro-nanobubbles, nanodroplets, and metal and metal oxide nanoparticles.<sup>5</sup> Metallic and inorganic nanoconstructs such as gold,<sup>6</sup> titanium dioxide (TiO<sub>2</sub>),<sup>7</sup> magnetite (Fe<sub>3</sub>O<sub>4</sub>)<sup>8</sup> and porous silicon nanoparticles<sup>9</sup> are believed to be promising sonosensitisers for future anticancer therapy. Their enormous surface area can be modified with functional

School of Cancer & Pharmaceutical Sciences, King's College London, UK.  
E-mail: maya.thanou@kcl.ac.uk

groups for various therapeutic applications and their submicrometer size allows them to penetrate deeply into tissues and be taken up efficiently by cells.<sup>6</sup> SDT might be useful for nanodroplet applications. However, this review will focus on the development of phase changing nanodroplets. Other nanoparticles used in SDT can be further referred from a review published by Canavese *et al.*<sup>5</sup>

Traditional UCAs are gas-filled microparticles with acoustic properties, *i.e.*, the ability to produce echogenicity from acoustic exposures, widely known as microbubbles.<sup>10</sup> The first generation of microbubbles was Alunex®, an echo-enhancer with an air core and a shell constructed with protein albumin. Highly echogenic contrast agents can majorly amplify ultrasound signals even in a low contrast medium, such as blood.<sup>11</sup> However, microbubbles have several disadvantages which restrict their application in the clinic. The size of microbubbles is around 1–10 µm, which confines their distribution in the vascular space, and limits the *in vivo* circulation time to a few minutes as they are rapidly cleared *via* the liver.<sup>12</sup> To overcome these problems, nanodroplets have been developed in the last two decades.<sup>12</sup> When compared to microbubbles, nanodroplets have advantages which make them more desirable for clinical application.<sup>13</sup>

Nanodroplets are composed of a stabilising shell and a perfluorocarbon core. The core remains liquid at body temperature but vaporises into microbubbles under ultrasound. PCNDs can enhance the extravasation of therapeutic agents into a target tissue site under ultrasound-induced ADV and subsequent acoustic cavitation.<sup>14</sup> To further understand the mechanism of ADV, the vapour pressure equilibrium between the liquid and gas phases in the core region of PCNDs is an aspect to be observed and characterised. Vapourisation takes place when the vapour pressure in the liquid phase of volatile liquids such as perfluorocarbons is increased above the surrounding gas phase pressure. What ultrasound does is that it can reduce the pressure surrounding PCNDs below the vapour pressure of the liquid perfluorocarbons encapsulated in the core region of the PCNDs. This results in liquid perfluorocarbon vapourisation, leading to the generation of microbubbles.<sup>15</sup> Nanodroplets are 10-fold smaller than microbubbles and able to pass through endothelial gaps and accumulate in the tumour site or lesions. The *in vivo* dwell time of nanodroplets is also prolonged for up to 4–5 hours, which offers potential to better target cancers.<sup>7</sup> Besides, the selection of the perfluorocarbon core offers nanodroplets ultrasound-responsive tuneable properties and high precision.<sup>13,16,17</sup>



**Weiqi Zhang**

*Weiqi Zhang is currently a PhD candidate at King's College London, under the supervision of Dr Maya Thanou. Her research is focused on nanoparticles as a contrast enhancement agent for MR imaging. She holds an MSc in Pharmaceutical Technology from King's College London and a BSc from Beijing University of Chinese Medicine.*



**Maya Thanou**

*Maya Thanou is Reader at the Institute of Pharmaceutical Science, King's College London. Prior to that she was a Dorothy Hodgkin Royal Society Research Fellow at Imperial College London, at the Department of Chemistry and the Genetic Therapies Centre, working in the area of cancer genetic therapies. In her current post she is focusing her research in the area of responsive nanoparticles for image guided therapy.*

*Dr Thanou has achieved research funding over £2.5 M during the last few years. She is the author of 80 peer reviewed papers and chapters. She is the editor of the RSC book Theranostics and Image Guided Drug Delivery. Her work has been selected by King's Commercialisation Institute as one of the best 6 projects in the institute. She is the key inventor of 9 patents, all in the area of formulation and drug delivery. She is the co-founder of AJMMed-i-caps, a start-up developing combination technologies (electronics and nanoparticles) for early colorectal cancer detection, and Apeikon Therapeutics, which develops image guided thermo-responsive nanoparticles for cancer drug delivery. She chairs the BBSRC LIDo Impact Industry Internships 3I committee. She is the science communicator of the Microwave Hyperthermia (MyWave) European Network. In 2019 she became Industry Trustee and a management committee member for the British Society for Nanomedicine.*

The pioneering work on nanodroplets was initiated by Apfel through the design of perfluorocarbon droplets that can vaporise into microbubbles under ultrasound irradiation.<sup>18</sup> Nanodroplets started to gain more attention and the number of publications has been increasing each year (Fig. 1). PCNDs can be combined with ultrasound technologies to produce local cavitation that can be used for contrast enhancement, tumour ablation, antivasular therapy and release of therapeutic agents loaded in nanodroplets.<sup>19</sup> Different applications of PCNDs are achieved by adjusting the ultrasound parameters.<sup>20</sup> Stable or inertial cavitation can be achieved depending on the intensity, amplitude and frequency of the ultrasound wave.<sup>3</sup> At low frequencies and low intensities, stable cavitation could produce strong echoes for imaging, but PCNDs need different ultrasound frequencies for vaporisation and imaging.<sup>21</sup> Microstreaming produced during stable cavitation could also temporarily enhance the permeability of physiological barriers such as BBB (blood-brain barrier) and endothelium.<sup>22</sup> Higher amplitude and lower frequency can be used for therapy application encompassing sonoporation and sonodynamic therapy.<sup>22,23</sup> At high intensity, including HIFU (high intensity focused ultrasound), PCNDs can also be used for histotripsy and tumour ablation.<sup>21</sup> The choice of ultrasound frequency and intensity settings used in previous studies for both diagnosis and therapy is summarised in Loskutova's review.<sup>21</sup>

Although there are no clinically approved nanodroplets in the market, there are several clinically approved microbubbles used in a wide variety of biomedical applications.<sup>25</sup> PCNDs' clinical prospect looks promising as they have a similar ability of contrast enhancement to that of microbubbles but they are superior to microbubbles. However, the drawback of nanodroplets is that they cannot be imaged before being acoustically activated by ultrasound.<sup>26</sup> To solve this problem, multimodal imaging nanodroplets can be developed by incorporating different imaging probes, for example, fluorescence imaging, magnetic resonance imaging (MRI) and positron emission tomography (PET).<sup>13</sup> In summary, these formulations are gaining attention as the amount of research increases which will push the clinical and commercial translation of this novel transformable nanoparticle.

This review aims to present the development of PCNDs for imaging and therapy purposes, focusing on chemical compositions and characteristics. Although an important topic, the chemistry of the components of these nanodroplets has not been discussed or reviewed yet. Therefore, we have provided examples of various chemical characteristics of nanodroplets while linking them with their efficiency as ultrasound/multimodal imaging agents as well as cavitation mediators. Cavitation can promote drug delivery through sonoporation (stable cavitation) or through jetting (inertial cavitation). The nanodroplet composition could be a strong attribute to this effect.

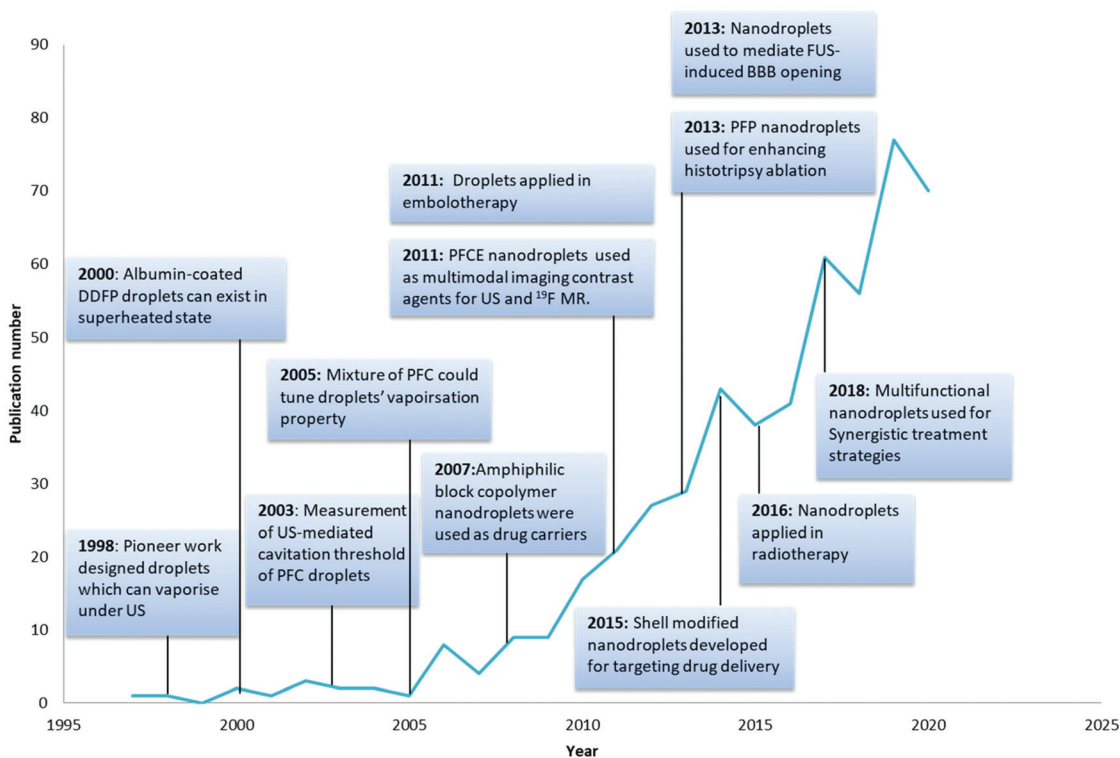


**Fig. 1** Milestones in the development history of nanodroplets<sup>18,27–35</sup> and number of publications related per year (search from the web of science Clarivate Analytics using keywords: perfluorocarbon nanodroplets, perfluorocarbon droplets, phase change nanodroplets and phase-change contrast agents).

## 2. Chemical composition of nanodroplets

Nanodroplets are composed of two parts: an encapsulation shell and core filled with liquid perfluorocarbon (PFC). The formulation is critical as it will influence the properties of the nanodroplets. The shell must be designed to maintain droplets' shape and original diameter after intravenous injections, as well as being able to expand into bubbles upon ADV.<sup>10</sup> The actual surface tension of nanodroplets is largely dependent on the state of the shell. The low-boiling point perfluorocarbons can remain liquid as a superheated state at physiological temperatures due to Laplace pressure provided by the shell.<sup>3</sup> Laplace pressure is a force generated by the surface tension at the interface of the shell and PFC core. Therefore, nanodroplets remain stable *in vivo* until sufficient acoustic energy is induced to promote vaporisation through ADV<sup>13</sup> (Fig. 2).

Different type of perfluorocarbons could also influence the vapourisation property and thermal stability of droplets.<sup>36</sup> Optimising the perfluorocarbon core could develop more precisely tuneable droplets with maximum performance in each application.<sup>28</sup> The property of the shell and core which influence the nanodroplet characteristics will be discussed later. Apart from the shell and core, drug encapsulation or/and droplet decoration (*e.g.*, imaging probe, targeting ligand) might be performed inside the liquid perfluorocarbon core, embedded in the shell or attached to the shell surface depend-

ing on the molecular weight and lipophilicity. These substances could also influence the acoustic property of nanodroplets.

### 2.1 Phase change nanodroplet shell composition

The choice of nanodroplets' shell is based on the criterion to find a balance between mechanical resistance to provide enough Laplace pressure and compliance to enable large deformation during ADV (Fig. 2).<sup>13</sup> Lacour *et al.* built a mathematical model to study the influence of hyperelastic shells on droplets' acoustic properties.<sup>38</sup> They concluded that the most favourable droplets' shell elastic properties correspond to soft materials, with a low value of shear modulus ( $G$ ) and high non-linearity ( $\beta$ ).  $G$  is the rheological property related to a material's response to shear stress; nonlinearity is significant as it corresponds to the large deformation of the shell.<sup>38</sup> Currently, commonly used shell materials include surfactants, albumin, lipids, and synthetic polymers<sup>13</sup> (Table 1). Among all the studies, lipids and polymers are the most popular material to form the droplets' shell. Lipids and fluorinated surfactants are considered as soft-shell materials whereas polymers and proteins are considered as hard-shell materials.<sup>39</sup> The advantages and disadvantages of each material are listed in Table 2.

Albumin is a pioneer shell used in both microbubble and nanodroplet formulation. It has been used extensively in fabricating droplets due to its ability to stabilise the surface of the droplets.<sup>27</sup> This material could thicken at the droplet state and thin to form ideal bubble shells upon vaporisation.<sup>40</sup> Most albumin-coated nanodroplets were prepared using sonication.<sup>25</sup> Among these studies, the albumin commonly used is bovine serum albumin (BSA)<sup>41,42</sup> and denatured BSA.<sup>24</sup> The albumin shell can also be modified. For example, Chang *et al.* loaded sonosensitizer IR780 iodine through hydrophobic interactions with albumin;<sup>24</sup> the surface of the shell could also be functionalised for the molecular targeting of specific biological targets.<sup>43</sup>

Surfactants have been explored to form stable microbubbles, but for nanodroplets, fluorosurfactants appear to be more favourable.<sup>13,39</sup> Although perfluorocarbon and alkane emulsifiers are both hydrophobic, surfactants still exhibit a very low affinity for perfluorocarbons.<sup>44</sup> Therefore, droplets fabricated with normal surfactants are not very stable.<sup>45</sup> To solve this stability issue, the approach is to replace the lipophilic hydrocarbon part of the emulsifier with a fluoro-philic perfluorocarbon part to make a fluorinated surfactant.<sup>44</sup> For example, a commercially available fluorosurfactant-Zonyl® (surface tension at 20 °C 16–23 mN m<sup>-1</sup>) has been used in a few studies.<sup>46,47</sup> A low surface tension fluorosurfactant could provide appropriate stabilisation for droplets against coalescence phenomena.<sup>39</sup>

Lipids are frequently used in biodegradable and biocompatible nanoparticle formulations. Lipid-based nanoparticles such as liposomes are one of the most useful carriers used for biomedical imaging and drug delivery because different mixtures can be easily formulated and modified in lipid-coated particles.<sup>25,48</sup> Lipids are successfully adopted in the fabrication

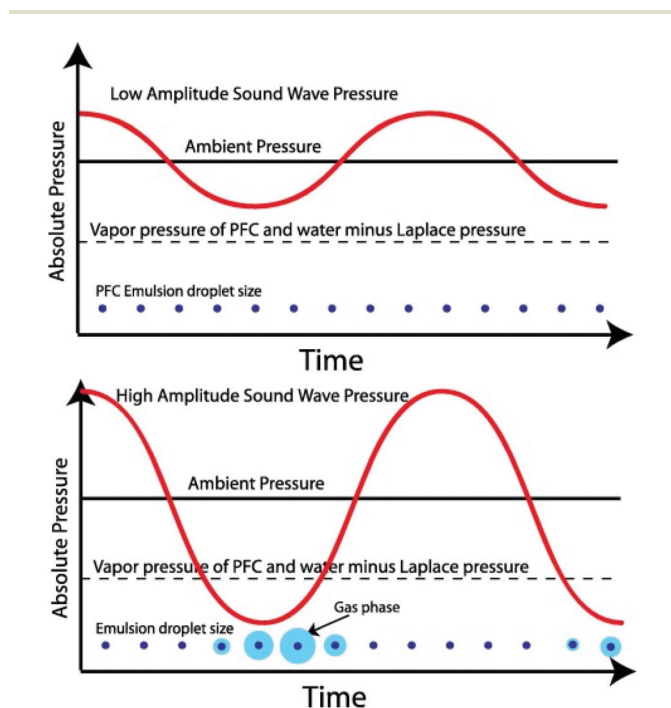
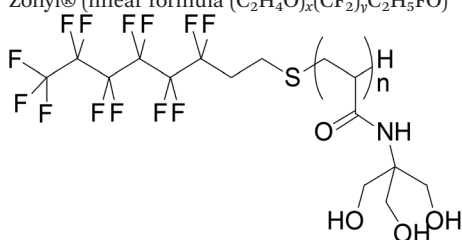


Fig. 2 Schematic of an ultrasonic acoustic wave in a perfluorocarbon emulsion. The graphs show emulsion droplets (not to scale) that only vaporise into the gas phase when the acoustic pressure is below the Laplace pressure<sup>37</sup> (this figure has been reproduced from ref. 37 with permission from Elsevier, copyright 2014).

**Table 1** Commonly used shell materials in nanodroplets

| Shell type | Material   | References  |
|------------|--|---|
| Protein    | Albumin  | Zhang <i>et al.</i> <sup>64</sup><br>Kripfgans <i>et al.</i> <sup>27</sup>  |
| Polymer    | PLGA: poly (lactic-co-glycolic acid)   | Giesecke <i>et al.</i> <sup>40</sup><br>Pisani <i>et al.</i> <sup>65</sup>  |
|            | PCL: polycaprolactone  | Astafyeva <i>et al.</i> <sup>66</sup><br>Rapoport <i>et al.</i> <sup>67</sup><br>Ji <i>et al.</i> <sup>68</sup>   |
| Lipids     | Chitosan   | Magnetto <i>et al.</i> <sup>69</sup>  |
|            | PLA: poly (lactic acid)  | Wei <i>et al.</i> <sup>70</sup>   |
|            | PDA: polydopamine  | Mannaris <i>et al.</i> <sup>58</sup>  |
|            | DPPC (1,2-dipalmitoyl- <i>sn</i> -glycero-3-phosphocholine)  | Zhang <i>et al.</i> <sup>64</sup>   |
|            | DPPA (1,2-dipalmitoyl- <i>sn</i> -glycero-3-phosphate monosodium salt)   | Zhang <i>et al.</i> <sup>64</sup>   |
| Surfactant | DSPC (1,2-distearoyl- <i>sn</i> -glycero-3-phosphocholine)   | Sheeran <i>et al.</i> <sup>71</sup>   |
|            | DSPE-PEG <sup>2000</sup> (1,2-distearoyl- <i>sn</i> -glycero-3-phosphoethanolamine- <i>N</i> -methoxy(polyethyleneglycol)-2000)                                    | Yarmoska <i>et al.</i> <sup>54</sup><br>Sheeran <i>et al.</i> <sup>71</sup>   |
|            | Cholesterol<br>Lecithin<br>Zonyl® (linear formula (C <sub>2</sub> H <sub>4</sub> O) <sub>x</sub> (CF <sub>2</sub> ) <sub>y</sub> C <sub>2</sub> H <sub>5</sub> FO) | Yarmoska <i>et al.</i> <sup>54</sup><br>Schad <i>et al.</i> <sup>49</sup><br>Schad <i>et al.</i> <sup>49</sup><br>Williams <i>et al.</i> <sup>47</sup><br>Astafyeva <i>et al.</i> <sup>44</sup> |

**Table 2** Advantages and disadvantages of different shell materials<sup>50,57</sup>

| Material    | Advantages   | Disadvantages  |
|-------------|--|--|
| Albumin     | Easy preparation method  | More rigid than other materials  |
| Surfactants | Fluoro-surfactants could provide appropriate stabilisation for droplets against coalescence phenomena  | Alkane surfactants show a low affinity for perfluorocarbons<br>May require considerable peak negative pressures to induce vaporisation   |
| Lipids      | Different mixtures can be easily formulated and modified in lipid shells   | A hydrophobic mismatch between the lipids may inevitably lead to lateral phase separation  |
| Polymers    | The polymer could facilitate the loading of drugs with high loading efficiency in the shell<br>Polymer nanodroplets possess a high surface to volume ratio so the rate of adsorption (on what?) is enhanced, and the kinetics of the reaction is accelerated<br>Polymer shell could act as an effective tool for targeting infections and wounds | Upon vaporisation, bubbles formed are highly unstable due to the presence of gas molecules within the polymer shell<br>Estimation of long-term shelf-life is difficult. Defects in the outer shell may result in the leaking of perfluorocarbon before reaching the target site<br>Acoustic threshold is higher than lipids or surfactants formulated nanodroplets |

of ultrasound-responsive droplets due to their elasticity.<sup>28,49</sup> One major advantage of the lipid shell is it has good mechanical flexibility which contributes to its ability to expand and collapse repeatedly.<sup>50</sup> Such properties ensure that the PCND is stabilised against dissolution and coalescence.<sup>13</sup> Most of the studies considered lipids to form a monolayer shell on nanodroplets. Chattaraj *et al.* used Transmission Electron Microscopy (TEM) to examine the shell property of nanodroplets, and the image shows a uniform texture of lipid monolayer (Fig. 3a).<sup>51</sup> However, Mountford *et al.* showed microscopy evidence that the nanodroplets prepared using microbubble condensation may have one or more bilayer lamella structures

(Fig. 3b).<sup>52</sup> They propose that the lipid monolayer could fold into bilayer folds upon compression or self-healing, and bilayer folds can then deform into the monolayer upon expansion (Fig. 3c).<sup>53</sup> The state of lipids on nanodroplets still needs more studies to explore.

The lipid composition could play a tuning role in the acoustic property of nanodroplets. Although numerous studies used lipid formulated nanodroplets, only a few studies have investigated the effect of the lipid shell composition on nanodroplets' size distribution and acoustic property.<sup>51,54</sup> Mountford *et al.* used a series of lipids with acyl chain lengths ranging from C14 to C20 to form nanodroplets. The results showed

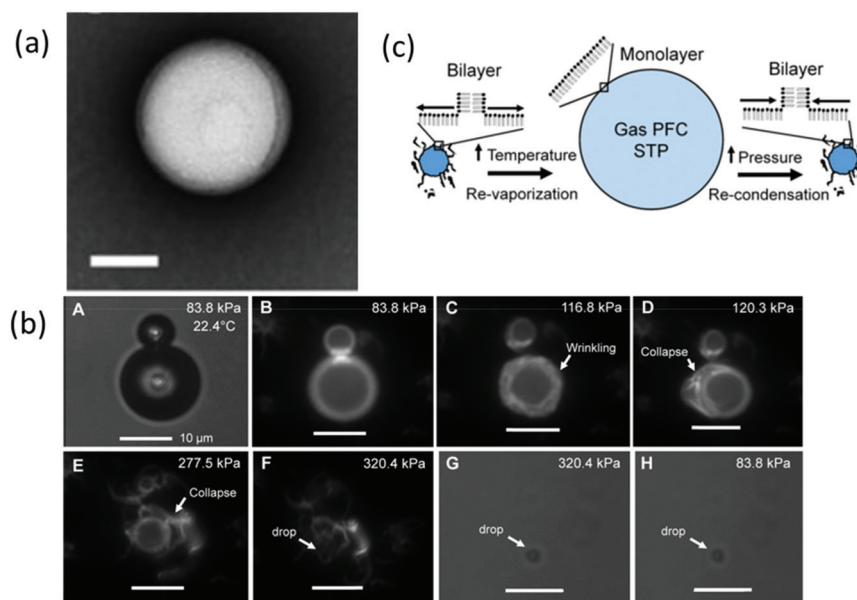


**Fig. 3** (a) TEM images of 4 v/v% PFH droplets, scale bar = 100 nm (shell: DPPC/PEG 1.3 mM/40 Mm in TBS)<sup>51</sup> (this figure has been reproduced from ref. 51 with permission from Royal Society of Chemistry, copyright 2011); (b) microscopy images of Dil, DSPC : DSPE-PEG2000 (9 : 1)-coated microbubbles undergoing condensation, the image shows sinuous lipid collapse structures<sup>52</sup> (this figure has been reproduced from ref. 52 with permission from American Chemical Society, copyright 2014); (c) schematic of microbubble-condensed nanodroplets with the lipid shell during vaporisation and condensation<sup>53</sup> (this figure has been reproduced from ref. 53 with permission from American Chemical Society, copyright 2015).

that energy needed to reach the vaporisation threshold increases linearly with the acyl chain length of lipids, which indicated that the lipid intermolecular cohesion force plays an important role for slowing the vaporisation process of nanodroplets.<sup>53</sup> A recent study by Chattaraj *et al.* suggested nanodroplets with a mixture of 40% DOPC, 40% DPPC with 20% cholesterol as the shell have ten times higher ultrasound contrast to DPPC-only formulation.<sup>51</sup> Besides, lipid-shelled nanodroplets are commonly coated with hydrophilic block polymers, usually poly (ethylene oxide) (PEG) chains. PEGylation is a typical approach to reduce non-specific cellular uptake and prolong blood half-life for nanocarriers.<sup>55</sup> For nanodroplets, PEGylation can not only influence biological behaviour, but also size and acoustic response. Increasing the molar percentage of PEGylated lipid reduces the average size and size variation of nanodroplets, and facilitates ultrasound imaging contrast in a murine model of breast cancer.<sup>54</sup> The influence of the PEG chain length was also addressed by Melich *et al.* They prepared 90% DPPC nanodroplets with 10% DSPE-PEG5000 or DSPE-PEG2000 using the microfluidics method. They concluded that there was no significant impact on the nanodroplet formulation quality under their operating parameters.<sup>39</sup>

Amphiphilic block copolymers as the shell material for nanodroplets could facilitate the loading of lipophilic drugs with high loading efficiency,<sup>13</sup> combining tumour-targeting, enhancing intracellular drug delivery as well as enhancing the ultrasound contrast properties.<sup>56</sup> Different types of polymers are used in the formulation of nanodroplets, including PLGA (poly (lactic-*co*-glycolic acid), PCL (polycaprolactone), chitosan, PLA (poly (lactic acid) and PDA (polydopamine).<sup>57,58</sup> PEG is

mostly used in combination with other polymers for size reduction and targeted drug delivery. Gao *et al.* had shown that the count rate value (corresponding to the concentration) of nanodroplets without PEG loads decreases significantly in solution containing serum due to protein aggregation with nanodroplets. However, nanodroplets that are modified with PEG could remain stable under the same conditions.<sup>59</sup> PLGA is a widely used biocompatible polymeric carrier with extended release property for loaded drug.<sup>57</sup> Cao *et al.* has loaded doxorubicin (DOX) into PLGA-coated nanodroplets and the drug-releasing profile shows that the drug was continuously released from nanodroplets without LIFU (low-intensity focused ultrasound) but burst drug release was observed after LIFU exposure.<sup>60</sup> Chitosan is a cationic linear polysaccharide extracted from marine animals. Its physicochemical properties such as nontoxicity, hydrophilicity, biocompatibility, biodegradability and high resistance to heat make it suitable for biomedical application.<sup>57</sup> Baghbani *et al.* prepared curcumin-loaded chitosan-stabilised nanodroplets for curcumin smart delivery and this formulation shows good curcumin entrapment efficiency (77.8%) due to high affinity between chitosan and curcumin.<sup>61</sup>

Most polymer-shelled nanodroplets load drugs in the polymer shell and the drug loading capacity is dependent on the concentration of the polymer.<sup>57</sup> The perfluorocarbon/copolymer ratio is also important for nanodroplet formulation. As, when the perfluorocarbon/copolymer is low, perfluorocarbon dissolved in the core of the micelle and no nanodroplets exist; with the increasing ratio of perfluorocarbon to polymer more nanodroplets are formed leading to droplet stabilisation and

micelles disappearing.<sup>62</sup> For microbubbles, decreasing the initial thickness of the copolymer shell could facilitate encapsulated drug transferring from the bubble to the neighbouring cells.<sup>63</sup> The influence of the polymer shell thickness of nanodroplets has not been investigated but we could hypothesize that this will influence the drug releasing profile of nanodroplets. And it was hypothesised that gaps between polymer molecules become larger on the nanodroplet shell after they change phase and this could facilitate drug release from the polymer shell.<sup>60</sup>

Several studies have reported that polymer-coated nanodroplets have higher stability and vaporisation threshold compared with lipid-coated nanodroplets. Melich *et al.* prepared nanodroplets with different shell materials, and the polymer shell (PLGA) showed better stability than lipid shell (DPPC: DSPE-PEG<sup>2000</sup>) nanodroplets. The results indicated PLGA coated nanodroplets exhibit good storage stability in the fridge (5 °C) over 1 month without any impact on the size and polydispersity, whereas lipid shell nanodroplets lack stability after storage probably due to vesicle aggregation.<sup>39</sup> The study by Cao *et al.* indicated that polymer-based (PLGA shell) nanodroplets need higher ultrasound energy to be activated into microbubble compared with lipid-based (DPPC, DPPG, DPPE, and cholesterol) nanodroplet formulation due to the stiffness of the polymer material.<sup>60</sup>

## 2.2 The core composition

The liquid core chosen for nanodroplets is preferably hydrophobic, bioinert and able to circulate safely in the body before being vaporised into a gas, *i.e.*, have an appropriate boiling point. Thus, unlike microbubbles which are normally formed using air, nitrogen or sulphur hexafluoride as the core, nanodroplets use perfluorocarbon to meet these criterias.<sup>3</sup> The perfluorocarbon family differs in chain length, giving rise to unique boiling points (Table 3).<sup>13</sup> After injection, perfluorocarbon released in blood fluid would be expected to be eliminated through the lungs. Perfluorocarbons have low partition coefficients in blood, so perfluorocarbons binding to blood proteins would be expected to be minimal.<sup>67</sup> The physicochemical properties of perfluorocarbons make them an attractive candidate for ADV, and Laplace pressure provided by the shell could allow them to remain stable within nanodroplets at body temperature until vaporised by sufficient acoustic energy.<sup>38</sup> The PFC concentration could also influence the size of nanodroplets. Ferri *et al.* indicated increasing the volumetric concentration of PFP from 5% to 15% v/v will lead to double size larger nanodroplets.<sup>72</sup>

The dodecafluoropentane DDFP (C<sub>5</sub>F<sub>12</sub>) was the first-ever studied droplet core from the early 2000s.<sup>27</sup> Even though the boiling point of DDFP (C<sub>5</sub>F<sub>12</sub>) is 29 °C, which is lower than body temperature, the superheated DDFP droplets could remain stable and circulate freely *in vivo* until activated by ultrasound due to the existence of Laplace pressure.<sup>30</sup> However, studies also showed that decreasing the size could increase vaporisation thresholds of perfluorocarbon droplets,<sup>73</sup> so nanodroplets with highly volatile perfluorocarbon,

*e.g.*, decafluorobutane DFB (C<sub>4</sub>F<sub>10</sub>) and octafluoropropane OFP (C<sub>3</sub>F<sub>8</sub>), were developed. This allows droplets with a size below 200 nm to be formed. These small size PCND can passively accumulate in the targeted tumour tissue.<sup>74</sup> In addition, nanodroplets with volatile perfluorocarbons play an important role in the diagnostic applications (ultrasound imaging) because a low boiling point core induces the droplets to have an earlier vaporisation.<sup>21</sup> Other perfluorocarbons also offer different advantages. For example, the boiling temperature of perfluorocarbon ether (PFCE) (C<sub>10</sub>F<sub>20</sub>O<sub>5</sub>) is 146 °C. Compared with DDFP, PFCE has a higher boiling point, therefore, has greater storage ability than DDFP. At the same time, activating the phase transition in PFCE nanodroplets requires only a slightly higher acoustic energy than those for DDFP confirmed in the experiment.<sup>16</sup> PFCE is also a fluorine-19 MR (magnetic resonance) imaging contrast agent with high sensitivity which could be used in image tracking<sup>75</sup> because PFCE contains 20 equivalent <sup>19</sup>F nuclei that generate a single resonance peak in <sup>19</sup>F MRI.<sup>16</sup>

Early studies focused on developing nanodroplets used single perfluorocarbons as the core. Kawabata *et al.* first used a mixture of DDFP and DFP as the droplet core to reduce the vaporisation threshold.<sup>28</sup> A perfluorocarbon mixing is a valuable tool to manipulate the thermal stability and the vaporisation threshold of droplets simultaneously to maximise the performance for specific applications.<sup>36</sup> Melich *et al.* then discovered that the ADV threshold of nanodroplets elevated with the increase of the PFH percentage in a liquid core made up of the PFH and PFP mixture.<sup>39</sup> Perfluorocarbon mixing is not limited to perfluorocarbons that exist in the same state (gas or liquid), but on the feasibility to mix across different states to produce tuneable droplets which are “flexible” for clinical applications.<sup>28</sup>

Apart from perfluorocarbons, adding other particles into nanodroplets could also influence vaporisation properties. For example, quantum dots are used as cavitation seeds in nanodroplets by mixing them into the perfluorocarbon solution.<sup>76</sup> Quantum dots could be visualised in fluorescence imaging and lower the vaporisation threshold.<sup>77</sup> Loading iron oxide nanoparticles within nanodroplets' inner surface of the shell could also reduce the vaporisation threshold.<sup>78</sup>

Currently, most of the studies have only fabricated phase-shift nanodroplets with a core composed of a single kind of perfluorocarbon and the number of studies using the mixture of perfluorocarbon as the core is limited. However, the perfluorocarbon mixture tends to offer more ideal properties to phase-shift nanodroplets such as a reduced vaporisation threshold and changeable composition for clinical use. Hence, in the future, the perfluorocarbon mixture is supposed to be developed as an essential part of phase-shift nanodroplets.

There are numerous studies indicating that the nanodroplet composition exhibits effects on their behaviour, but most of the studies focused on evaluating nanodroplets' properties in aqueous buffer or water settings. It is essential to highlight that nanodroplets possess different characteristics either the *in vitro* or *in vivo* ambiances. To date, only several studies have

Table 3 Summary of perfluorocarbons used in various phase change nanodroplets

| Compound name   | Molecular formula*                             | IUPAC name*  | Chemical structure* | Molecular weight* (g mol <sup>-1</sup> ) | Boiling point* (°C) | References   |
|---|--|--|---------------------|--|---------------------|--|
| Octafluoropropane (OFP)                               | C <sub>3</sub> F <sub>8</sub>                  | 1,1,1,2,2,3,3,3-Octafluoropropane  |                     | 188.02                                   | -39                 | Sheeran <i>et al.</i> <sup>50</sup><br>Doinikov <i>et al.</i> <sup>82</sup>  |
| Perfluorobutane (FPB)/<br>decafluorobutane (DFB)      | C <sub>4</sub> F <sub>10</sub>                 | 1,1,1,2,2,3,3,3,4,4,4-Decafluorobutane   |                     | 238.03                                   | -36.7               | Chen <i>et al.</i> <sup>32</sup><br>Matsunaga <i>et al.</i> <sup>74</sup><br>Doinikov <i>et al.</i> <sup>82</sup><br>Kawabata <i>et al.</i> <sup>28</sup>  |
| 2 <i>H</i> ,3 <i>H</i> -Decafluoropentane (DFP)       | C <sub>5</sub> H <sub>2</sub> F <sub>10</sub>  | 1,1,1,2,2,3,4,4,5,5,5-Decafluoropentane  |                     | 252.05                                   | 55                  | Vlaisavljevich <i>et al.</i> <sup>83</sup><br>Li <i>et al.</i> <sup>84</sup><br>Miles <i>et al.</i> <sup>85</sup><br>Kripfgans <i>et al.</i> <sup>27</sup><br>Giesecke <i>et al.</i> <sup>40</sup><br>Vlaisavljevich <i>et al.</i> <sup>83</sup><br>Strohm <i>et al.</i> <sup>86</sup><br>Giesecke <i>et al.</i> <sup>40</sup> |
| Perfluoropentane (PFP)/<br>dodecafluoropentane (DDFP) | C <sub>5</sub> F <sub>12</sub>                 | 1,1,1,2,2,3,3,4,4,5,5,5-Dodecafluoropentane  |                     | 288.03                                   | 29                  | Vlaisavljevich <i>et al.</i> <sup>83</sup><br>Li <i>et al.</i> <sup>84</sup><br>Miles <i>et al.</i> <sup>85</sup><br>Kripfgans <i>et al.</i> <sup>27</sup><br>Giesecke <i>et al.</i> <sup>40</sup><br>Vlaisavljevich <i>et al.</i> <sup>83</sup><br>Strohm <i>et al.</i> <sup>86</sup><br>Giesecke <i>et al.</i> <sup>40</sup> |
| Perfluorohexane (PFH)                                 | C <sub>6</sub> F <sub>14</sub>                 | 1,1,1,2,2,3,3,4,4,5,5,6,6-Tetradecafluorohexane  |                     | 338.04                                   | 58                  | Vlaisavljevich <i>et al.</i> <sup>83</sup><br>Li <i>et al.</i> <sup>84</sup><br>Miles <i>et al.</i> <sup>85</sup><br>Kripfgans <i>et al.</i> <sup>27</sup><br>Giesecke <i>et al.</i> <sup>40</sup><br>Vlaisavljevich <i>et al.</i> <sup>83</sup><br>Strohm <i>et al.</i> <sup>86</sup><br>Giesecke <i>et al.</i> <sup>40</sup> |
| Perfluoromethylcyclohexane (PFM)                      | C <sub>7</sub> F <sub>14</sub>                 | 1,1,2,2,3,3,4,4,5,5,6,6-Undecafluoro-6-(trifluoromethyl)cyclohexane                              |                     | 350.05                                   | 76                  | Vlaisavljevich <i>et al.</i> <sup>83</sup><br>Li <i>et al.</i> <sup>84</sup><br>Miles <i>et al.</i> <sup>85</sup><br>Kripfgans <i>et al.</i> <sup>27</sup><br>Giesecke <i>et al.</i> <sup>40</sup><br>Vlaisavljevich <i>et al.</i> <sup>83</sup><br>Strohm <i>et al.</i> <sup>86</sup><br>Giesecke <i>et al.</i> <sup>40</sup> |
| Perfluorooctane (PFO)                                 | C <sub>8</sub> F <sub>18</sub>                 | 1,1,1,2,2,3,3,4,4,5,5,6,6,7,7,8,8-Octadecafluorooctane   |                     | 438.06                                   | 105.9               | Fabilli <i>et al.</i> <sup>42</sup>  |
| Perfluorodichlorooctane (PFD)                         | C <sub>8</sub> Cl <sub>2</sub> F <sub>16</sub> | 1,1-Dichloro-1,2,2,3,3,4,4,5,5,6,6,7,7,8,8-hexadecafluorooctane                                  |                     | 470.97                                   | 176                 | Lanza <i>et al.</i> <sup>87</sup>  |
| Perfluoro-15-crown-5-ether<br>(perfluorocarbonE)      | C <sub>10</sub> F <sub>20</sub> O <sub>5</sub> | 2,2,3,3,5,5,6,6,8,8,9,9,11,11,12,12,14,14,15,15-Icosafluoro-1,4,7,10,13-pentaoxacyclopentadecane |                     | 580.07                                   | 146                 | Rapoport <i>et al.</i> <sup>56</sup><br>Rapoport <i>et al.</i> <sup>75</sup>   |

\*Values taken from Pubchem.



evaluated nanodroplets' characteristics in serum/blood-mimicking fluid. Serum could slightly influence the stability of nanodroplets. Meng *et al.* has incubated polymer shell nanodroplets in buffer solution containing 10% fetal bovine serum (FBS) at 37 °C where the particle size only increased slightly within 24 h.<sup>79</sup> Other studies showed that the nanodroplet size remains stable in serum, which indicates that nanodroplets could possess good stability under physiological conditions, even for nanodroplets with a low-boiling point PFC such as PFP.<sup>58–60</sup> Besides, fluid viscosity and environmental parameters also affect nanodroplets' acoustic property. Rojas *et al.* has compared the vaporisation threshold of nanodroplets in phosphate-buffered saline (PBS, viscosity = 1 cP) and a blood-mimicking fluid (viscosity = 5.4 cP). The result indicated that increasing the viscosity has a significant effect on nanodroplets' vaporisation threshold in a 30 mm tube.<sup>80</sup> They also suggested that the increase of the vaporisation threshold in *in vivo* rather than *in vitro* experiments was due to boundary constraints and hydrostatic pressure derived from the tissue and capillary walls, as well as the high blood fluid viscosity.<sup>80</sup> Helfield *et al.* has shown that fluid viscosity may influence the fragmentation and acoustic emission of lipid-shell microbubbles although not a similar research has been conducted on nanodroplets.<sup>81</sup> Unfortunately, with limited numbers of studies relating to nanodroplet characterisation in biological fluids, existing studies have suggested that the *in vitro* studies should evaluate nanodroplets in different media before transitioning into *in vivo* studies.

### 3. Phase change nanodroplet preparation techniques

A variety of techniques has been developed to manufacture nanodroplets, including sonication, homogenisation, extrusion, microfluidics, and microbubble condensation. Different preparation methods could influence the property of nanodroplets, especially their size and size uniformity. As mentioned earlier, nanodroplets have a smaller size than conventional microbubbles, which allows them have advantages like prolonged *in vivo* circulation and deep penetration into the tissues *via* the extravascular space. Their nano-scale size also allows them to passively accumulate in tumour tissue due to the EPR (Enhanced Permeability and Retention) effect. The nanodroplet size also influences their acoustic properties. For micron-sized droplets, the acoustic activation threshold depends on the initial diameter (Fig. 4).<sup>73</sup> It was reported that vaporisation thresholds are reduced with increasing droplet size.<sup>88</sup> Although data for nanosized droplets do not exist yet, it appears that the size is a critical parameter for the activation pressure threshold. The size distribution also influences the acoustic performance of nanodroplets.<sup>50</sup> Polydisperse droplets will not respond the same under ultrasound energy.<sup>89</sup> To improve the uniformity of activation, the most important thing is to use techniques that can create nanodroplets with low polydispersity.<sup>36</sup> It is important to choose an appropriate

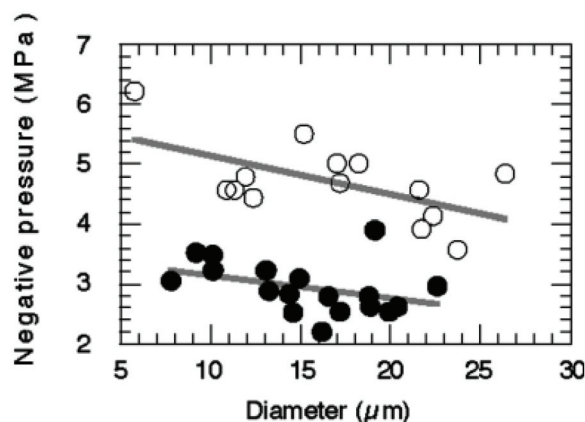


Fig. 4 Relationship between the pressure threshold for ADV and diameter of nanodroplets. Decreasing the droplet diameter will increase pressures for vaporisation<sup>73</sup> (this figure has been reproduced from ref. 73 with permission from Royal Society of Chemistry, copyright 2004).

method for preparing nanodroplets according to their desired properties for future application, either for imaging or drug delivery.

#### 3.1 Agitation/homogenisation

Some of the earliest reports related to PCND mention production by agitation. The methods vary from simply shaking by hand to commercial homogenisation systems,<sup>18,90</sup> with protocols varying significantly. In general, these methods produce droplets first by mixing the shell components with an aqueous solution and then adding perfluorocarbon and homogenising into emulsions. Since the entire droplet solution is within a single container, agitation techniques could avoid material losses. However, these methods often produce droplets with a wide size distribution and low reproducibility.<sup>13</sup>

#### 3.2 Sonication

Sonication is a common and simple method to produce nanoparticles including nanodroplets. In previous studies, both a sonication bath<sup>62</sup> and probe sonicator<sup>47,77,91</sup> were used. In this method, the component of droplets (shell material and perfluorocarbon) is emulsified by ultrasound in a continuous aqueous phase/buffer solution (Fig. 5). Usually, the vial must be kept in an ice bath during sonication to prevent excess heating.<sup>50</sup> The parameters of sonication also influence the property of nanodroplets. Ferri *et al.* have studied the influence of the power and duration of sonication on nanodroplets. The result shows that a longer sonication time and sonication intensity leads to a lower size and size dispersity.<sup>72</sup>

The main advantage of this method is the ease of use and low cost. Besides, this method could avoid material loss compared with some flow techniques because the emulsion system is closed. This technique is also applicable to incorporate other agents (*e.g.*, solid nanoparticles) into nanodroplets. However, the disadvantage of this method is the relatively low nanodroplet uniformity. Gao *et al.* used a sonication bath, and

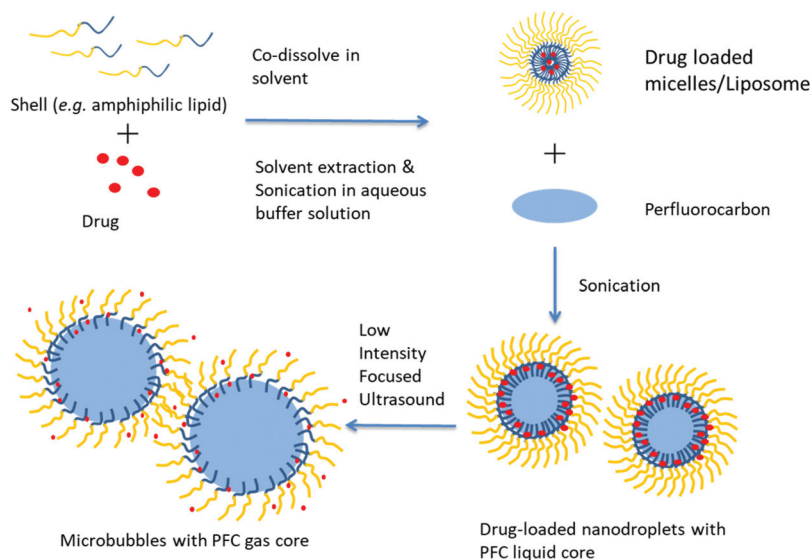


Fig. 5 Schematic representation of the preparation of PCND and their phase change with focused ultrasound.

the final product is a mix of nanodroplets with micelles.<sup>62</sup> Sheeran *et al.* also showed an example of the increased polydisperse size distribution of probe-sonicated nanodroplets.<sup>50</sup> In addition, erosion of the probe tip also has the potential to contaminate the nanodroplet solution with metals during preparation. That's why it is very important to inspect the tip to avoid any defect on its surface.<sup>50</sup>

### 3.3 Extrusion

Extrusion was used for the preparation of liposomes and may now also be adopted to fabricate nanodroplets.<sup>86,89</sup> Extrusion is commonly used in combination with other approaches (*e.g.*, sonication, condensation) instead of using alone. Sheeran *et al.* fabricated nanodroplets using a 1  $\mu\text{m}$  porous membrane filter. The shell material was first dried in the vial to form a thin film and hydrated with a buffer solution. DFB ( $\text{C}_4\text{F}_{10}$ ) was added to the lipid suspension mixed with glycerol in a cold room. Then the solution was extruded at  $-5\text{ }^\circ\text{C}$  to avoid freezing of the aqueous solution and maintain the liquid state of the DFB.<sup>89</sup>

Compared with sonication, extrusion has higher monodispersity. However, extrusion did not appear to be capable of manufacturing submicron droplets regardless of the membrane size used, maybe due to the low perfluorocarbon surface tension and the very high viscosity of the phospholipid solution at  $-5\text{ }^\circ\text{C}$ .<sup>17</sup> Besides, extrusion is more complex than sonication. For phospholipid formulated nanodroplets, extrusion may preferentially form liposomes instead of droplets.<sup>50</sup>

### 3.4 Microbubble condensation

Preparing nanodroplets by microbubble condensation first appeared in the literature due to the challenge of producing liquid nanoscale droplets from highly volatile perfluorocarbon (*e.g.*, DFB, OFP) which exist as a gas at room temperature.<sup>88</sup> In the method, microbubbles with a volatile perfluorocarbon core

ideal for ultrasound interaction are generated and then the gaseous precursors are condensed into liquid state droplets by cooling and applying pressure.<sup>92</sup> Once the liquid core is formed, the reduction in size results in a submicron distribution of droplets, and the Laplace pressure could stabilise the droplets against re-expansion at room temperature until the nanodroplets are activated by ultrasound or increased temperature.<sup>36</sup> Microbubble condensation will generate liquid core nanodroplets instead of gas core nanobubbles.

This method has several advantages.<sup>36,50</sup> First, it offers a method to generate a high concentration of nanodroplets of volatile compounds simply.<sup>50</sup> Second, microbubbles' condensation could manipulate functionalised droplets at the micro-scale before microbubbles were condensed. It is relatively simple to incorporate particles, dyes and targeting ligands into the droplet shell.<sup>71,93</sup> Third, since this method begins from a population of microbubbles ideal for imaging, if condensation and vaporisation proceed optimally, after vaporisation, nanodroplets could become bubbles with an ideal size.<sup>36</sup> Finally, this technique provides an opportunity to produce nanodroplets directly from well-developed microbubbles. Research related to microbubbles is earlier than nanodroplets. There are many publications related to novel microbubbles applied in molecular imaging and drug/gene delivery, and these modifications can be applied directly into droplets with microbubble condensation.<sup>50</sup>

However, there are some drawbacks. First, as most microbubbles tend to be polydisperse,<sup>94</sup> preparing droplets with a narrow size distribution is difficult.<sup>50</sup> Second, although it is simple to incorporate components into the droplet shell, it is difficult to encapsulate components into the perfluorocarbon core due to phospholipid shedding during condensation and the condensation of microbubbles can be impeded by the low purity of perfluorocarbon.<sup>52</sup>

### 3.5 Microfluidics

Microfluidic technologies offer a promising route to produce uniform emulsions. Microfluidics for forming droplets can be either passive or active (Fig. 6). In a passive microfluidic device, an aqueous phase (continuous phase) was injected into the first inlet cartridge, whereas the organic phase (usually ethanol or acetonitrile solvent) containing dissolved perfluorocarbon and a coating material (dispersed phase) is injected into the second inlet *via* a pressure-driven flow.<sup>95</sup> The two phases meet at a junction, at which the perfluorocarbon liquid extends to form a 'figure' or 'jet' and eventually pinched off to form a droplet.<sup>96</sup> The speed of the organic phase and aqueous phase pumped through the two separate microfluidic cartridges are different.<sup>39</sup> The particles size can be controlled by altering the flow rate ratio of the two phases.<sup>36</sup> In most studies, nanodroplets are manufactured using the passive method. Compared with passive techniques, active techniques modulate droplet formation with the aid of additional energy input. Droplet generation can be manipulated by two strategies: first by introducing additional forces from electrical, magnetic, and centrifugal controls; second by modifying viscous, inertial, and capillary force by varying intrinsic parameters like flow velocity and material properties.<sup>95</sup>

Microfluidics presents a powerful approach to optimising current formulations of nanodroplets. The advantage of this method is it allows for monodisperse size distributions; therefore, activation thresholds are highly uniform and the vaporisation efficiency is increased.<sup>50</sup> It is also worth mentioning that this advantage also offers an opportunity to characterise the physical aspects of emulsions. An experimental relation-

ship between the particle size and vaporisation temperature could be tested to estimate the Laplace pressure as well as surface tension.<sup>36</sup> However, there are some disadvantages. The ease and speed of manufacturing droplets are limited.<sup>13</sup> Microfluidics requires specialised equipment which is relatively expensive and not easy for novice users. It is even more challenging to produce nanoscale droplets. It either needs nanofluidic devices,<sup>97</sup> or combines microfluidics with condensation.<sup>98</sup>

### 3.6 Spontaneous nucleation

A novel method for producing nanodroplets using spontaneous nucleation, also called the OUZO method, was demonstrated by Li *et al.*<sup>152</sup> Lipid surfactants, or any other stabiliser, are first dissolved in an organic solvent. They first prepared an initial lipid-ethanol stock solution. Perfluorocarbons were dissolved in the stock solution until it was fully saturated and adjusted with a stock solution to achieve the desired percentage. Finally, the aqueous solvent was added to the solution to reduce the solubility of lipid and perfluorocarbon, forcing droplets to spontaneously nucleate.<sup>152</sup> A stabiliser can be added to increase the stability of nanodroplets. This method is easy to operate but not commonly used in the literature.

## 4. Phase change nanodroplets for bioimaging

Nanodroplets allow simultaneously therapeutic and diagnostic application. Unlike microbubbles, which are unable to enhance image contrast outside blood vessels, nanodroplets can migrate through hyperpermeable vessel walls in tumours and accumulate in the interstitial tissue.<sup>99</sup> Another advantage of droplets is that they can retain their nano-scale size in the bloodstream, enabling them to circulate longer. Nanodroplets with liquid cores can be converted to gas bubbles, which make them good contrast agents for ultrasound imaging.<sup>21</sup>

Ultrasound imaging is a broadly used imaging technique for real-time, non-ionising, high frame-rate imaging with low cost.<sup>100</sup> Ultrasound contrast agents are a good tool to investigate sites of inflammation and solid tumour due to the highly permeable vascular networks in these tissues<sup>74</sup> (Fig. 7). The vaporisation of nanodroplets results in acoustic emissions, which are usually observed by B-mode (Brightness) ultrasound probe.<sup>27,61,62</sup> However, in the beginning, nanodroplets that use perfluorocarbon compounds with a boiling point above room temperature<sup>61</sup> (*e.g.*, DDFP, PFH) need a significant amount of acoustic energy to vaporise, making diagnosis and molecular imaging with nanodroplets especially difficult.<sup>74</sup> Therefore, nanodroplets using highly volatile perfluorocarbons were developed later, which are inherently more sensitive to acoustic energy.<sup>88</sup> Apart from this, acoustic imaging could also monitor the size of bubbles through harmonic emissions produced by vaporised nanodroplets.<sup>99</sup>

However, unlike microbubbles, nanodroplets remain inert and virtually undetectable by conventional ultrasound imaging

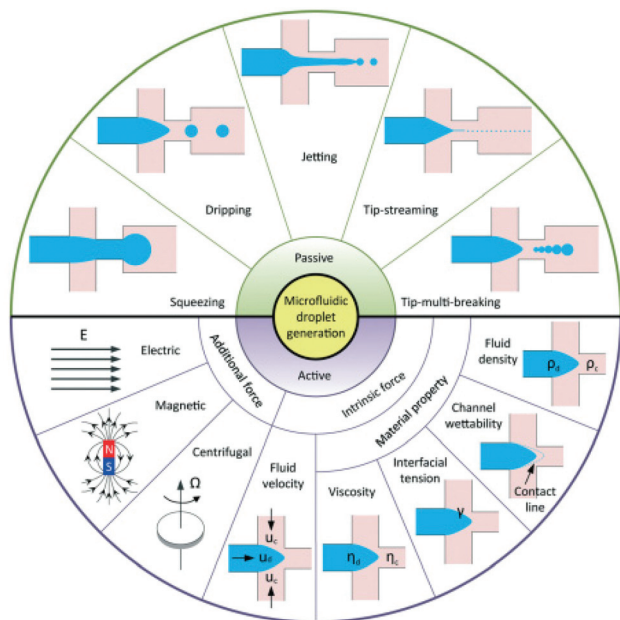


**Fig. 6** Schematic of droplet generation in passive and active methods<sup>95</sup> (this figure has been reproduced from ref. 95 with permission from Royal Society of Chemistry, copyright 2001).

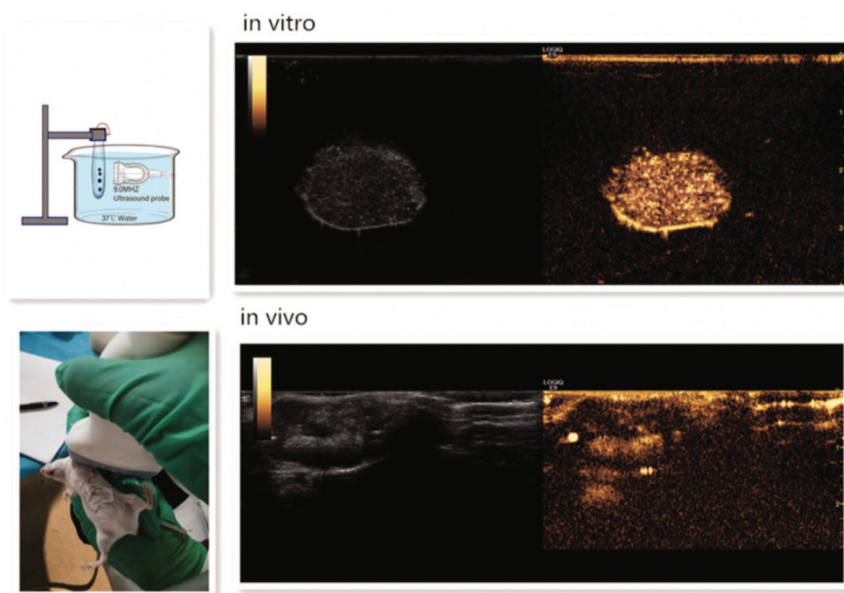


Fig. 7 Ultrasound enhancement images of nanodroplets *in vitro* and *in vivo*<sup>101</sup> (this figure has been reproduced from ref. 101 with permission from Taylor & Francis, copyright 2020).

before vaporisation.<sup>12</sup> Besides, the ultrasound as an imaging tool has poor tissue discrimination ability compared with MRI and largely depends on the analysis of the operator.<sup>102</sup> Thus, another imaging system can be used to assist in guiding the focused ultrasound.<sup>13</sup> Different imaging probes are added to nanodroplets to make them into multimodal imaging contrast agents. Multimodal imaging nanodroplets will become a future developing direction because other imaging tools could offset the weakness of nanodroplets and work in correlation with ultrasound. The core and shell of nanodroplets can be adopted to make particles detectable under other kinds of imaging *e.g.*, fluorescence/MRI/PET/X-ray.<sup>77,103</sup> Since each type of imaging has its advantages and disadvantages, different imaging modalities are generally considered complementary rather than competitive.

Photoacoustic (PA)/ultrasound (US) imaging is a hybrid biomedical imaging technique. It combines the contrast superiority of optical imaging with the resolution superiority and deep tissue penetration of ultrasound imaging.<sup>104</sup> Nanodroplets used for PA/US imaging are prepared by adding a photo-absorber in the nanodroplet formulation.<sup>105</sup> This dual-modality agent can undergo vaporisation induced by ultrasound energy or optical energy by laser activation<sup>106</sup> and produce high US/PA contrast on demand. After absorbing optical energy, the photo-absorber in nanodroplets produces heat and photoacoustic pressures, which lead to the liquid-to-gas phase transition of perfluorocarbon core. The activation process of nanodroplets by optical energy is called ODV (optical droplet vaporisation) instead of ADV.<sup>104</sup>

One unique property of laser-activated nanodroplets is they can vaporise and recondense with different perfluorocarbon core compositions. When nanodroplets are formed with a per-

fluorocarbon core with a low-boiling point which is lower than body temperature (37 °C), they remain gas phase after vaporisation and not able to condense back to liquid droplets. However, if nanodroplets are formulated with a high-boiling point perfluorocarbon like perfluorohexane, they can recondense back to liquid droplets from gaseous bubbles, which allows repeat activation and deactivation (Fig. 8).<sup>107</sup> Worth mentioning is that the repeat activation and deactivation of nanodroplets is not only controlled by the perfluorocarbon core, but a combination of several parameters including particle size, laser fluence, amount of dye and imaging conditions.<sup>106</sup> Therefore, a thoughtful choice of parameters is necessary to design the recondensation of nanodroplets.

Apart from the perfluorocarbon core, the photoabsorber is also an important parameter for a PA contrast agent. The laser activation and photoabsorber vary based on clinical needs. Laser activation in the near-infrared region was used in several studies by adding ICG (indocyanine green) and plasmonic nanoparticles in nanodroplets, because in this region the optical penetration is effective.<sup>105</sup> ICG is an FDA approved commonly used intravenous dye to measure cardiac output, hepatic function and for ophthalmic angiography in clinics with rare side effects. The study of Hannah *et al.* reported PA/US nanodroplets by loading ICG in an albumin shell and the sample can be irradiated with a 780 nm wavelength laser pulse.<sup>108</sup> Hannah *et al.* encapsulated gold nanorods in nanodroplets consisting of a BSA shell and PFP core. Upon pulsed laser irradiation at 780 nm, liquid perfluorocarbon undergoes phase transition yielding giant photoacoustic transients and the gaseous phase provides ultrasound contrast enhancement. After vaporisation, the PA signal decayed but still existed. At this stage, the PA signal originates from expelled nanorods

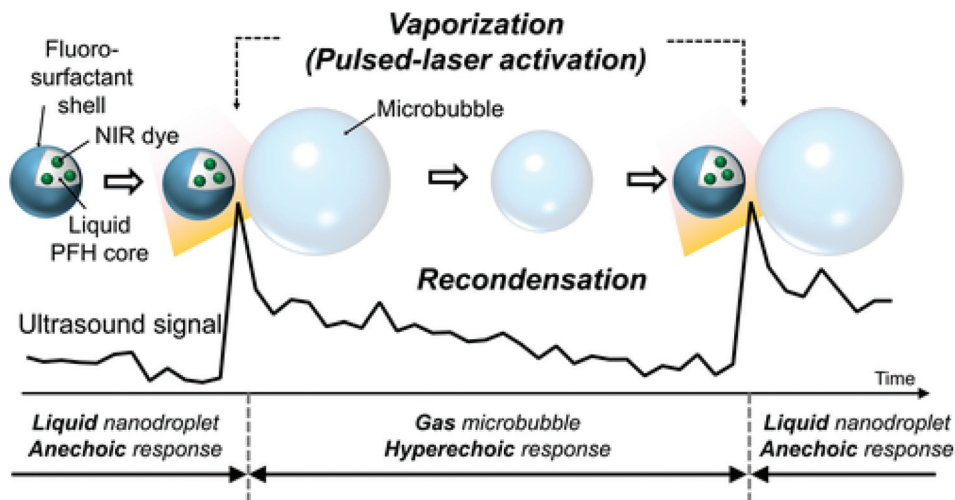


**Fig. 8** Vaporisation and recondensation of laser-activated nanodroplets. When activated, nanodroplets immediately produce strong ultrasound signals<sup>107</sup> (this figure has been reproduced from ref. 107 with permission from John Wiley and Sons, copyright 2017).

and endogenous thermal expansion.<sup>43</sup> The laser pulse with 1064 nm wavelength is also a commonly used optical source for PA/US dual-modality imaging. The advantages of using 1064 nm light for biomedical imaging are it can improve contrast due to minimal absorption by blood-perfused tissue, and this laser source is inexpensive.<sup>105</sup> Santiesteban *et al.* loaded coated copper sulfide nanoparticles (CuS NPs) in a PFP core and the nanodroplets have good PA/US contrast as well as good biocompatibility over other metallic particles.<sup>109</sup> Photoabsorbers can also be encapsulated on nanodroplet shells. Santiesteban *et al.* prepared two nanodroplets with different photoabsorber dyes on a lipid shell, and these nanodroplets can be activated by 680 nm and 1064 nm laser pulse separately.<sup>110</sup>

Fluorescence imaging is imaging with high sensitivity but is only semi-quantitative and has poor tissue penetrating ability. Currently, most fluorescence labelled droplets are used for *in vitro* and preclinical studies, especially for optimising droplets for further human injection.<sup>77</sup> Gorelikov *et al.* suspended CdSe/ZnS core/shell quantum dots (QDs) in the perfluorocarbon core of droplets for rapid, preclinical optical assessment.<sup>77</sup> To understand the condensation process of microbubble to nanodroplets, Mountford *et al.* added fluorescent lipid DiI into the membrane of microbubbles to visualise their deformation during pressurisation under fluorescence microscopy.<sup>52</sup>

MRI is an accurate imaging tool for soft tissue anatomy with high spatial resolution but low sensitivity. Conversely, ultrasound is an imaging technique with high sensitivity but low spatial resolution. Besides, unlike ultrasound which can provide real-time monitoring, MRI needs a relatively long imaging time for high-resolution imaging.<sup>103</sup> Therefore, ultrasound and MRI are combined as a compliment in many clinical applications.<sup>102</sup> Previous studies adopted nanodroplets into *T2*-weighted contrast agents by loading superpara-

magnetic iron oxide nanoparticles (SPIO NPs) or  $\text{Fe}_3\text{O}_4$ .<sup>111–113</sup> SPIO NPs have been loaded into the shell of nanodroplets by the interaction between aliphatic terminated SPIO NPs and lipid to form a stable monolayer shell.<sup>112</sup> SPIO could greatly improve nanodroplets' liquid-to-gas phase change efficiency upon ultrasound exposure and make the nanodroplets magnetically responsive. SPIO loaded droplets have the potential to be manipulated *via* an external magnetic field which is highly advantageous for drug delivery in the previous work.<sup>78</sup> Recently, some studies focus on adopting nanodroplets into *T1*-weighted contrast agents.<sup>114</sup> Other nanoparticles, like liposomes and micelles, have been adopted into MRI contrast agents by incorporating ligand onto the macromolecular membrane to increase the gadolinium ion payload. The same method can be used in nanodroplets. Maghsoudinia *et al.* has embedded a small molecular contrast agent Gadovist into the alginate polymer shell of nanodroplets. Nanodroplets show a higher *T1*-weighted MRI signal than free molecule Gadovist.<sup>114</sup>

As fluorinated compounds can be monitored by  $^{19}\text{F}$  (fluorine) MR spectroscopy, nanodroplets loaded with PFCE or PFOB (perfluorooctyl bromide) in the core were used as multi-modal contrast agents directly for ultrasound and  $^{19}\text{F}$  MRI.<sup>75</sup> Lanza and Wickline's team has conducted a series of studies on PFCE and PFOB nanoemulsions as  $^{19}\text{F}$  MR contrast agents.<sup>115–117</sup> Apart from adding an MRI probe into nanodroplets, changes in proton resonance frequency could be used to monitor temperature changes under MR thermometry. Crake *et al.* used MR thermometry to measure the thermal effects induced by vaporising DDFP lipid-coated nanodroplets.<sup>118</sup>

PET is one of the most effective techniques to quantify the agents in preclinical models and patients.<sup>119</sup> Adapting nanodroplets to be detectable by PET could allow understanding of the pharmacokinetics and biodistribution of nanodroplets, which is very important for developing a safe and efficient drug carrier.<sup>120</sup> Amir *et al.* prepared PET contrast nanodroplets

by dissolving [ $^{18}\text{F}$ ]CF<sub>3</sub>(CF<sub>2</sub>)<sub>7</sub>(CH<sub>2</sub>)<sub>3</sub>F into a PFOB core.<sup>121</sup> Contrast-enhanced digital mammography (CEDM), as one of the techniques of X-ray mammography, can provide good sensitivity and specificity in breast cancer detection and characterisation. Hill *et al.* used PFOB nanodroplets as CEDM contrast agents because the bromine atom in the molecule has good X-ray attenuation characterisation.<sup>122</sup>

Imaging of nanodroplets is important not only because it can be used as imaging contrast agents, but also enable us to understand the *in vivo* stability, biodistribution and pharmacokinetics of nanodroplets. However, few studies have investigated these aspects of nanodroplets. Rapoport *et al.* have tested the pharmacokinetics of polymer-coated nanodroplets by measuring the PFCE core using  $^{19}\text{F}$  MRI. The result indicated that 40 to 50% were still circulating 2 h after the injection and after 24 h most signals were found from the liver.<sup>29</sup> Pre-clinical biodistribution and pharmacokinetics are essential for the future development of nanodroplet. PET, MR and fluorescence imaging have great potential to be used in these studies. Fluorescence imaging can be used for short-term real-time biodistribution imaging in small animals<sup>123</sup> whereas PET imaging has clinical translatability for large animals and human. Besides, PET allows treatment monitoring and planning.<sup>121</sup>

## 5. Development of sonoresponsive nanodroplets for drug delivery

The combination of therapeutic ultrasound and microbubbles is broadly used in the medical area while the large size has become an inevitable restriction for microbubbles to extravasate beyond the blood vessels and significantly constrained their therapeutic efficacy.<sup>124</sup> Compared to microbubbles, nano-sized droplets with a superior *in vivo* stability tend to have a broader therapeutic application such as in ablation, embolotherapy and drug delivery which are listed in Table 4.<sup>64,83,125</sup>

Histotripsy, a novel ablation method, can fractionate the tumour tissues in a non-invasive manner by taking advantage of the cavitation generated by the high-pressure ultrasound.<sup>31</sup> The ultrasound frequencies used in currently approved clinical application are normally below 1 MHz.<sup>21</sup> However, this approach is unable to handle tumours with micrometastases and small nodules as they are challenging to be visualized before operation.<sup>83</sup> Nanodroplets as cavitation nuclei can reduce the threshold of cavitation and the introduction of nanodroplets into histotripsy can realize the selective and targeted tumor ablation as the nanodroplets are capable of penetrating tumor vasculature and accumulating into tumors.<sup>126</sup> Embolotherapy is another method, suppressing the tumor outgrowth through ischaemic damage.<sup>64</sup> The microbubbles converted from nanodroplets under the stimulation of ultrasound have a diameter larger than blood vessels, resulting in the occlusion of blood vessels and blocking the blood flow in the tumor site to induce the shrink of tumors.<sup>30</sup> Currently, the development of this therapeutic approach is still in the pre-

clinical stage, and in order to get into clinical use, controlling the migration of these gas emboli to avoid arterial occlusion in healthy tissues and optimizing the ultrasound parameter to trigger the ADV efficiently are two challenges standing ahead.

To date, the preclinical research using sonoresponsive nanodroplets in drug delivery has been comparatively more diverse, covering chemotherapy, gene therapy, sonodynamic therapy, photo-thermal/dynamic therapy and the combination of them. The sonoresponsive nanodroplets will turn into microbubbles through the ADV process and the cavitation of these microbubbles in the blood can generate mechanical force such as shock waves and microfluids, causing the disruption of biological barriers through the perforation on cell membranes, thus enhancing the drug delivery where the mechanism is described in Fig. 9.<sup>3</sup>

For chemotherapy, most the recent studies loaded chemotherapy drugs on the shell of nanodroplets, and ultrasound could facilitate the phase change of nanodroplets as well as drug release. Baghbani *et al.*,<sup>127</sup> fabricated DOX-loaded nanodroplets using alginates as the outer shell and perfluorohexane (PFH) as the liquid core. Surfactant Tween 20 in this formulation could prevent the recognition of nanodroplets from the reticulo-endothelial system and prolong their half-life.<sup>127</sup> An increased biodistribution of DOX was discovered, from approximately 2  $\mu\text{g g}^{-1}$  in its free state to around 12  $\mu\text{g g}^{-1}$  in nanodroplets under sonication. Using a biocompatible material, for example, chitosan can ensure the safety of DOX-loaded nanodroplets.<sup>101</sup> No significant cellular structure impairment was found in functional organs, indicating that loading DOX inside this drug carrier could considerably mitigate its cardiotoxicity and nephrotoxicity, while the anti-tumour rate increases from 8.35% in the DOX control group to 39.50% in the DOX-loaded nanodroplet group, which revealed that DOX-loaded nanodroplets could offer a great potent in suppressing the tumour outgrowth.<sup>101</sup> Cao *et al.* discovered that nanodroplets composed of different outer shells required different ultrasound intensities to activate acoustic cavitation.<sup>60</sup> Hence, it is estimated that the co-delivery of nanodroplets composed of a lipid and polymer could enhance the delivery of chemotherapeutic agents to a large extent as the cavitation of lipid nanodroplets could facilitate the accumulation of polymer nanodroplets in tumors.<sup>60</sup>

The outer shell of nanodroplets can be modified by attaching various ligands to optimise their therapeutic performance. Zhao *et al.* managed to use this property to prepare a drug-loading nanodroplet with cell-penetrating and targeting capability.<sup>128</sup> The primary outer shell of this nanodroplet was composed of DPPC, DSPE-CPP and cholesterol, while the cargo loaded inside the nanodroplet was another anti-cancer drug named 10-hydroxycamptothecin (HCPT). Modifying the surface of the nanodroplets with transactivating transcriptional activator (TAT) protein, which facilitates the translocation of large molecules across the cellular membrane, could exploit the cell-penetrating capability of HCPT into the cytoplasm or nuclei.<sup>129</sup> And the addition of hyaluronic acid (HA) in this formulation could enhance the targeting capability of

Table 4 Recent preclinical studies using nanodroplets to deliver therapeutic agents

| Therapy             | Therapeutic agent                             | Outer shell   | Liquid core                                    | Delivery mechanism   | References                            |
|---------------------|---|---|--|--|---------------------------------------|
| Chemotherapy        | DOX   | Alginate, Tween 20  | PFH  | Nanodroplets can form microbubbles through the ADV process, and encapsulated DOX can be released through the cavitation triggered by ultrasound. The addition of Tween 20 prolongs the circulation time of nanodroplets <i>via</i> the avoidance of RES  | Baghbani <i>et al.</i> <sup>127</sup> |
|                     | DOX   | DPPC, DPPG, DPPE and cholesterol                          | PFH  | Both lipid and polymer nanodroplets can turn into microbubbles under the sonication of ultrasound, and the DOX can be released locally through the collapse of microbubbles. However, the polymer nanodroplets with a hard shell require a higher intensity of ultrasound to stimulate the ADV process                             | Cao <i>et al.</i> <sup>60</sup>       |
|                     | DOX   | mPEG-PLGA Chitosan  | PFH  | The chitosan nanodroplets can develop into microbubbles through the ADV process and release the DOX after the disruption of microbubbles. The use of biocompatible chitosan can improve the biosafety of this drug delivery system   | Zhou <i>et al.</i> <sup>101</sup>     |
|                     | HCPT  | DPPC, DSPE-CPPs, cholesterol, HA                          | PFH  | The nanodroplets modified with CPP can actively deliver the HCPT across the cellular membrane. The addition of HA can increase the targeting capability of nanodroplets through the binding of overexpressed CD44 in human hepatoma  | Zhao <i>et al.</i> <sup>128</sup>     |
|                     | HCPT  | DPPC, DSPE-PEG <sub>3400</sub> -tLyP-1, DPPG, cholesterol | PFH  | tLyP-1 is a homing-penetrating peptide binding to the neuropilin-1 receptor overexpressed in human tumour cells. The addition of tLyP-1 to the nanodroplets could enhance their penetration and accumulation into tumours  | Zhu <i>et al.</i> <sup>131</sup>      |
|                     | HCPT  | DSPE-PEG <sub>2000</sub> -FA, DPPG cholesterol            | PFH, Fe <sub>3</sub> O <sub>4</sub>            | The addition of FA binding to the overexpressed FA receptor in SKOV3 ovarian cancer cells can increase the targeting capability of nanodroplets. The Fe <sub>3</sub> O <sub>4</sub> acting as a contrast agent can improve the PAI of nanodroplets and realize the theranostic of cancers  | Liu <i>et al.</i> <sup>113</sup>      |
| Gene therapy        | Luciferase gene                               | PGA-g-PEG-AHNP  | PFH, C <sub>11</sub> F <sub>17</sub> -PAsp-DET | The use of AHNP on the nanodroplets binding to the overexpressed Her2/ <i>neu</i> receptor in breast cancer can improve the targeting capability of nanodroplets, and the peptide itself can have an anti-tumour efficacy. The amphiphilic core can help to condense the negatively charged genes into the nanodroplet efficiently | Gao <i>et al.</i> <sup>59</sup>       |
|                     | miRNA-139, miRNA-203a, miRNA-378a, miRNA-422a | DPPC, DSPE-PEG <sub>2000</sub> -NH <sub>2</sub>           | PFH  | These nanodroplets loaded with four different genes were intratumorally administered. The released gene <i>via</i> the ADV and cavitation process can have anti-tumour efficacy by inhibiting the PIK3 CA mutation in hepatoma cells   | Dong <i>et al.</i> <sup>133</sup>     |
| Sonodynamic therapy | IR780   | DPPC, DSPE-mPEG <sub>2000</sub> , cholesterol             | PFH  | The ADV process involved in the release of sonosensitizer IR780 could facilitate the leakage and accumulation of nanodroplets into tumours. Moreover, the loaded IR780 itself displayed a significant tumour penetration and mitochondria-targeting ability  | Zhang <i>et al.</i> <sup>144</sup>    |
|                     | HMME  | DPPC, DSPE-mPEG <sub>2000</sub> -FA, cholesterol          | PFH  | The sonosensitizer HMME was released through the ADV and cavitation process, which could disrupt the vasculature and enhance the penetration of HMME deep into the tumour. The addition of FA binding to the overexpressed FA receptor in the ovarian cells could enhance the targeting ability of nanodroplets                    | Yang <i>et al.</i> <sup>146</sup>     |

Table 4 (Contd.)

| Therapy                           | Therapeutic agent              | Outer shell                                     | Liquid core | Delivery mechanism   | References                        |
|-----------------------------------|--------------------------------|---|-------------|--|-----------------------------------|
| Photothermal therapy              | AuNP                           | Human serum albumin                             | DDFC        | The sonoporation caused by the cavitation of nanodroplets could enhance the delivery of AuNP into the tumour cells. The interaction between light and AuNP could increase the temperature of tumours and induce the apoptosis of tumour cells  | Liu <i>et al.</i> <sup>138</sup>  |
| Photodynamic therapy              | IR780                          | Lecithin, cholesterol, DSPE-PEG <sub>2000</sub> | PFH         | The dissolved O <sub>2</sub> in the liquid core (PFH) could ameliorate the hypoxia tumour environment, ensure the generation of cytotoxic ROS and enhance the therapeutic efficacy of photodynamic therapy   | Tang <i>et al.</i> <sup>139</sup> |
| Chemo-radiotherapy                | Cisplatin prodrug              | DPPC, DSPE-PEG <sub>5000</sub> , cholesterol    | DFCE        | The therapeutic outcome was caused by chemotherapy and radiotherapy. The use of nanodroplets in this study enhanced the delivery of chemotherapeutic agents, reduced its systematic toxicity, and the O <sub>2</sub> dissolved in the DFCE could help tackle the hypoxia in the tumours, thus amplify the impact of radiotherapy                           | Yao <i>et al.</i> <sup>147</sup>  |
| Chemo-antivascular therapy        | DOX                            | DPPC, DSPG, DSPE-PEG <sub>5000</sub>            | PFH         | The mechanical waves generated through the ADV of nanodroplets could disrupt the tumour vasculature and inhibit cell proliferation. The vascular disruption could also facilitate the diffusion of DOX into tumours and obtain an enhanced anti-tumour effect  | Ho <i>et al.</i> <sup>149</sup>   |
| Chemo-photothermal therapy        | Melanin, DOX                   | PVA   | PFH         | The loaded melanin was a photosensitizer which could trigger the vaporisation of PFH under laser irradiation and generate a photothermal therapeutic effect. The cavitation of nanodroplets could facilitate the penetration of DOX in tumours to have an enhanced chemotherapeutic effect   | Hu <i>et al.</i> <sup>150</sup>   |
| Photothermal/photodynamic therapy | ZnF <sub>16</sub> Pc molecules | PEG-based perylene diimide (PDI)                | PFH         | The outer shell of the nanodroplets was a photoabsorber which could increase the temperature of tumours and trigger the vaporisation of PFH under laser irradiation, while the O <sub>2</sub> dissolved in the liquid core could improve the photodynamic therapeutic outcome of a ZnF <sub>16</sub> Pc molecule which was a photosensitizer in this study | Tang <i>et al.</i> <sup>34</sup>  |
| Radiotherapy/photodynamic therapy | TaOx nanoparticles             | C18PMH-PEG                                      | PFH         | The TaOx nanoparticles decorated on the nanodroplets could enhance the therapeutic outcomes of radiotherapy and lead to the damage of DNA. The O <sub>2</sub> dissolved in the PFH was beneficial for radiotherapy and photodynamic therapy to generate abundant cytotoxic ROS and kill cancers  | Song <i>et al.</i> <sup>151</sup> |

nanodroplets by binding to the overexpressed cluster of differentiation (CD-44) in human hepatoma.<sup>130</sup> These elaborate nanodroplets under the irradiation of low-intensity focused ultrasound showed a three-fold increase in the mean tumour suppression rate compared to the free drug-treated group, from 29.17% to 94.97%, and displayed great potential in treating hepatoma. Following the same design route, a novel tumour homing-penetrating peptide tLyP-1 as an alternative to TAT was attached to the same lipid-based nanodroplets for deeper tumour penetration, and the enhanced accumulation of HCPT-loaded nanodroplets was discovered as well.<sup>131</sup> In another study, folic acid (FA) was attached to the surface of HCPT-loaded nanodroplets made up of DSPE-PEG2000, DPPG

and cholesterol.<sup>114</sup> FA could bind to the overexpressed FA receptor in SKOV3 tumour cells and is broadly used as a ligand to enhance the targeting capability of nanocarriers, increase the accumulation of therapeutic agents in tumours and mitigate their off-target possibility.<sup>132</sup> A significant increase in nanodroplet distribution and HCPT concentration was observed in the tumour. The adequate accumulation of therapeutic agents in tumours remarkably improved the tumour inhibitory rate to 73.6% compared to the control group.<sup>113</sup>

The cargo loaded in nanodroplets can not only be chemotherapeutic agents but also be therapeutic genes. Gao *et al.* prepared gene loaded nanodroplets to improve the gene transfection rate through the cavitation and sonoporation triggered



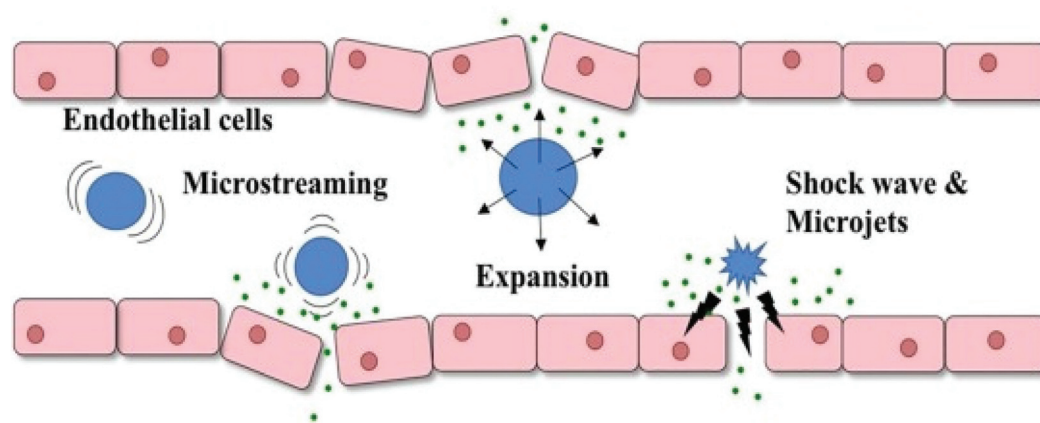


**Fig. 9** Schematic illustration of how UCAs respond to ultrasound which results in the increase of endothelial cell permeability. UCAs will oscillate and collapse under ultrasonic exposure, generating mechanical forces such as shock waves, microjets and microstreaming which temporarily disrupt endothelial cells and cause sonoporation<sup>3</sup> (this figure has been reproduced from ref. 3 with permission from Elsevier, copyright 2019).

by ultrasound.<sup>59</sup> The outer shell of the nanodroplets was fabricated by PGA-g-PEG-AHNP synthesised from  $\gamma$ -glutamic acid ( $\gamma$ -PGA) and PEG-AHNP. The core of this nanodroplet was made up of PFP and C<sub>11</sub>F<sub>17</sub>-PAsp-DET, (synthesized from C<sub>11</sub>F<sub>17</sub>, aspartate and diethylenetriamine). To optimise the targeting capability of this gene-loaded nanodroplet to breast cancer, anti-Her2/*neu* peptide (AHNP), which could bind to the overexpressed Her2/*neu* receptors in breast cancer, was modified to the surface of the nanodroplets. A dramatically improved gene expression was discovered in the mice intravenously and intratumoral administered with gene-loaded nanodroplets. Recently, four pre-microRNA plasmids (miR139, miR203a, miR378a and miR422a) downregulating the PIK3 CA mutation in hepatocellular carcinoma were loaded onto the positively charged surface of nanodroplets to investigate their anti-tumour potential.<sup>133</sup> The nanodroplets in this study were constructed using DPPC and DSPE-PEG2000-NH<sub>2</sub>. After the direct intratumoral injection of these four plasmid-loaded nanodroplets, inhibited tumour growth rate and prolonged survival time were discovered in these four groups after sonication, among which the pre-microRNA-139 group displayed the most outstanding therapeutic efficacy, with a four-time increase in the anti-tumour rate compared to the group treated with bare nanodroplets.

The mechanism involved in cancer treatment varies with the therapeutic agents. Aside from chemotherapy, photothermal or photodynamic therapy (PDT) can also treat a wide range of tumours. The mechanism of photothermal therapy is to induce the apoptosis of tumour cells *via* temperature elevation, while for PDT, the death of tumour cells attributes to the generation of reactive oxygen species (ROS) *via* the interaction between the photosensitizer and laser light.<sup>134,135</sup> Photosensitizers irradiated by light can transfer energy to oxygen, which can overcome tumor hypoxia and cause cell death.<sup>136</sup> Moreover, oxygen (O<sub>2</sub>) has superior solubility in liquid perfluorocarbon, turning the nanodroplet into an O<sub>2</sub> reservoir and enhancing the generation of cytotoxic ROS.<sup>137</sup>

Liu *et al.*, prepared Au nanoparticle (AuNP) loaded nanodroplets to amplify the anti-tumour efficacy of photothermal therapy.<sup>138</sup> The outer shell of the nanodroplets was made up of human serum albumin (HSA), and dodecafluorocarbon (DDFC) was used as the liquid core. When treated with AuNP loaded nanodroplets, sonication, and laser radiation, the tumour temperature could reach 50 °C, considerably higher than the other control groups. In terms of PDT, the therapeutic efficacy is hampered by hypoxia in tumours. As previously stated, nanodroplets can ameliorate this condition through the production of ROS.<sup>137</sup> A study compared the anti-tumour efficacy of IR780 loaded lipid nanodroplets with or without PFH, and a remarkably inhibited tumour outgrowth was discovered in the mice treated with IR780 and PFH encapsulated nanodroplets which indicated that the hypoxia of the tumour microenvironment could be adjusted by using the appropriate drug delivery system.<sup>139</sup>

Sonodynamic therapy (SDT) was developed recently as a novel treatment method for tumour. It damages cancer cells by ultrasound stimulation of a sonosensitizer.<sup>140</sup> The mechanism underlying the effects of SDT is not fully understood, but it is thought that acoustic cavitation induced by the interaction between ultrasound waves and the aqueous environment can activate sensitizers to transfer energy to nearby oxygen molecules, subsequently resulting in the formation of ROS. Compared with photodynamic therapy (PDT), SDT has higher tissue penetration because the sonosensitizer can be activated by low-intensity ultrasound whereas PDT uses light as a stimulator.<sup>5</sup> IR780 iodide has been used as a sonosensitizing agent to be encapsulated in ultrasound-responsive nanodroplets for SDT. This is a lipophilic, near-infrared fluorescence (NIRF) dye that does not only perform NIRF imaging but can effectively target organic-anion transporting polypeptides (OATPs) – commonly overexpressed in cancer cells.<sup>141–143</sup> Zhang *et al.* have fabricated this IR780-loaded nanodroplet.<sup>144</sup> The outcome of the *in vivo* biodistribution test revealed that encapsulating IR780 into the nanodroplet shell could enhance the accumu-

lation of IR780 to the tumours because of the EPR effect of nanodroplets and the mitochondria-targeting capability of IR780. When the mice were treated with pristine nanodroplets, a comparatively large amount of nanodroplets was discovered in the liver and spleen rather than the tumour. Moreover, the administration of IR780-loaded nanodroplets with ultrasound could significantly slow down the growth of tumours, indicating a promising potential of this treatment strategy. Another agent that has been evaluated is hematoporphyrin monomethyl ether (HMME) – an effective sonosensitizer with lower toxicity and higher singlet oxygen yield to cause cellular apoptosis through the mitochondrial apoptotic pathway.<sup>145</sup> In order to treat ovarian cancer, Yang *et al.* encapsulated HMME into the lipid shell of nanodroplets with perfluoropentane as core.<sup>146</sup> FA was conjugated to the surface of nanodroplets, targeting the overexpressed FA receptor in 90% of ovarian cancers.<sup>132</sup> The nanodroplets together with ultrasound also induced ROS formation, resulting in tumour necrosis and apoptosis. The tumour inhibitory rate was 87.68% higher than the control group, which firmly supports the potential utilisation of lipid-based nanodroplets to improve SDT efficacy in clinical studies.<sup>146</sup>

Synergistic treatment strategies have been introduced to strengthen the therapeutic outcomes by combining two or more single treatment strategies where nanodroplets can also display their ability to enhance therapeutic agents' delivery. For instance, liposomes with cisplatin prodrug encapsulated (cisPT-Lip) in chemoradiotherapy could further use PFCE as a liquid core to inhibit tumour outgrowth and significantly prolong the median survival time of treated mice by 6–8 days compared to the other control groups.<sup>147</sup> The PFCE with great O<sub>2</sub> loading capacity could increase the oxygenation in tumours, and this sufficient O<sub>2</sub> accumulation was essential for radiotherapy to cause DNA damage of tumour cells.<sup>148</sup> Chemotherapy has been integrated with anti-vascular therapy to inhibit tumour growth, where the ADV of DOX-loaded nanodroplets can disrupt the tumour vasculature, reduce cell proliferation, increase the distribution of DOX, and restrain the growth of tumours eventually.<sup>149</sup> Apart from these treatment strategies, many other preclinical studies have also taken advantage of nanodroplets in chemo/photothermal therapy, photo-dynamic/thermal therapy, and radio/photodynamic therapy to optimise drug distribution for a better anti-tumour efficacy.<sup>34,150,151</sup>

The application of sonoresponsive nanodroplets in drug delivery is in its developing state, and there is still a long way to go before getting into clinical use. Firstly, standard ultrasound protocols have not been set to effectively enhance drug delivery and cause minimal damage to peripheral tissues according to different diseases in patients. Secondly, immunotherapy as a rising star in the medical field has attracted great attention. Using sonoresponsive nanodroplets to deliver therapeutic agents and trigger immune response can be a new trend. Apart from these, exploring a new administration route for sonoresponsive nanodroplets, for example, intranasal delivery, may widen their application in the future.

## 6. Conclusion

Nanodroplets are novel nanoparticles for both diagnostic and therapeutic applications. In this review, the chemical composition and preparation methods were introduced and compared. Then applications of imaging and therapeutic applications of nanodroplets were summarised and how they were chemically adopted for different applications was highlighted. This review gives an overview of how to design nanodroplets according to their desired application.

Nanodroplets have great potential for future development. Although there have been no commercially available nanodroplets to date, recent research and the fact that nanodroplets are composed of safe and previously tested materials indicate that they have a great opportunity for application in the clinic. The therapeutic potential of nanodroplets is currently being explored and is demonstrating the extraordinary ability of tumour drug penetration and improved treatments in mouse models. However, the biodistribution and pharmacokinetic studies related to nanodroplets are limited and need more investigation. Besides, more preclinical studies are needed before nanodroplets are clinically approved. From a translation point of view, nanodroplets with good size uniformity and stability are needed.

## Conflicts of interest

There are no conflicts to declare.

## Acknowledgements

The authors are thankful for financial support from the King's-China Scholarship Council PhD Scholarship Programme.

## References

- 1 Z. Izadifar, Z. Izadifar, D. Chapman and P. Babyn, An introduction to high intensity focused ultrasound: Systematic review on principles, devices, and clinical applications, *J. Clin. Med.*, 2020, **9**, 1–22.
- 2 M. Thanou and W. Gedroyc, MRI-Guided Focused Ultrasound as a New Method of Drug Delivery, *J. Drug Delivery*, 2013, **2013**, 1–12.
- 3 A. L. Y. Kee and B. M. Teo, Biomedical applications of acoustically responsive phase shift nanodroplets: Current status and future directions, *Ultrason. Sonochem.*, 2019, **56**, 37–45.
- 4 E. P. Stride and C. C. Coussios, Cavitation and contrast: The use of bubbles in ultrasound imaging and therapy, *Proc. Inst. Mech. Eng., Part H*, 2010, **224**, 171–191.
- 5 G. Canavese, *et al.*, Nanoparticle-assisted ultrasound: A special focus on sonodynamic therapy against cancer, *Chem. Eng. J.*, 2018, **340**, 155–172.

- 6 A. Sazgarnia, A. Shanei, N. T. Meibodi, H. Eshghi and H. Nassirli, A novel nanosonosensitizer for sonodynamic therapy: in vivo study on a colon tumor model, *J. Ultrasound Med.*, 2011, **30**, 1321–1329.
- 7 K. Ninomiya, K. Noda, C. Ogino, S. I. Kuroda and N. Shimizu, Enhanced OH radical generation by dual-frequency ultrasound with TiO<sub>2</sub> nanoparticles: Its application to targeted sonodynamic therapy, *Ultrason. Sonochem.*, 2014, **21**, 289–294.
- 8 A. Ebrahimi Fard, A. Zarepour, A. Zarrabi, A. Shanei and H. Salehi, Synergistic effect of the combination of triethylene-glycol modified Fe<sub>3</sub>O<sub>4</sub> nanoparticles and ultrasound wave on MCF-7 cells, *J. Magn. Magn. Mater.*, 2015, **394**, 44–49.
- 9 A. P. Sviridov, *et al.*, Lowering of the cavitation threshold in aqueous suspensions of porous silicon nanoparticles for sonodynamic therapy applications, *Appl. Phys. Lett.*, 2015, **107**, 123107.
- 10 M. A. Borden, G. Shakya, A. Upadhyay and K. H. Song, Acoustic nanodrops for biomedical applications, *Curr. Opin. Colloid Interface Sci.*, 2020, **50**, 101383.
- 11 A. Zlitni and S. S. Gambhir, Molecular imaging agents for ultrasound, *Curr. Opin. Chem. Biol.*, 2018, **45**, 113–120.
- 12 C. Mannaris, *et al.*, Microbubbles, Nanodroplets and Gas-Stabilizing Solid Particles for Ultrasound-Mediated Extravasation of Unencapsulated Drugs: An Exposure Parameter Optimization Study, *Ultrasound Med. Biol.*, 2019, **45**, 954–967.
- 13 H. Lea-Banks, M. A. O'Reilly and K. Hynynen, Ultrasound-responsive droplets for therapy: A review, *J. Controlled Release*, 2019, **293**, 144–154.
- 14 C. De Gracia Lux, *et al.*, Novel method for the formation of monodisperse superheated perfluorocarbon nanodroplets as activatable ultrasound contrast agents, *RSC Adv.*, 2017, **7**, 48561–48568.
- 15 C. Y. Lin and W. G. Pitt, Acoustic droplet vaporization in biology and medicine, *BioMed Res. Int.*, 2013, **2013**, 404361.
- 16 N. Rapoport, Phase-shift, stimuli-responsive perfluorocarbon nanodroplets for drug delivery to cancer, *Wiley Interdiscip. Rev.: Nanomed. Nanobiotechnol.*, 2012, **4**, 492–510.
- 17 N. Rapoport, Drug-Loaded Perfluorocarbon Nanodroplets for Ultrasound-Mediated Drug Delivery, in *Therapeutic Ultrasound*, ed. J.-M. Escoffre and A. Bouakaz, Springer International Publishing, 2016, pp. 221–241. DOI: 10.1007/978-3-319-22536-4\_13.
- 18 R. E. Apfel, *Activatable infusible dispersions containing drops of a superheated liquid for methods of therapy and diagnosis*, 1998.
- 19 R. Guo, *et al.*, Functional ultrasound-triggered phase-shift perfluorocarbon nanodroplets for cancer therapy, *Ultrasound Med. Biol.*, 2021, **47**, 2064–2079.
- 20 S. Xu, *et al.*, Acoustic droplet vaporization and inertial cavitation thresholds and efficiencies of nanodroplets emulsions inside the focused region using a dual-frequency ring focused ultrasound, *Ultrason. Sonochem.*, 2018, **48**, 532–537.
- 21 K. Loskutova, D. Grishenkov and M. Ghorbani, Review on Acoustic Droplet Vaporization in Ultrasound Diagnostics and Therapeutics, *Wiley Interdiscip. Rev.: Nanomed. Nanobiotechnol.*, 2019, **2019**, 1–20.
- 22 R. Chandan, S. Mehta and R. Banerjee, Ultrasound-Responsive Carriers for Therapeutic Applications, *ACS Biomater. Sci. Eng.*, 2020, **6**, 4731–4747.
- 23 G. ter Haar, Therapeutic applications of ultrasound, *Prog. Biophys. Mol. Biol.*, 2007, **93**, 111–129.
- 24 N. Chang, *et al.*, IR780 loaded perfluorohexane nanodroplets for efficient sonodynamic effect induced by short-pulsed focused ultrasound, *Ultrason. Sonochem.*, 2019, **53**, 59–67.
- 25 S. R. Sirsi and M. Borden, Microbubble compositions, properties and biomedical applications, *Bubble Sci., Eng., Technol.*, 2009, **1**, 3–17.
- 26 E. Stride, *et al.*, Microbubble Agents: New Directions, *Ultrasound Med. Biol.*, 2020, **46**, 1326–1343.
- 27 O. D. Kripfgans, J. B. Fowlkes, D. L. Miller, O. P. Eldevik and P. L. Carson, Acoustic droplet vaporization for therapeutic and diagnostic applications, *Ultrasound Med. Biol.*, 2000, **26**, 1177–1189.
- 28 K. Kawabata, N. Sugita, H. Yoshikawa, T. Azuma and S. Umemura, Nanoparticles with Multiple Perfluorocarbons for Controllable Ultrasonically Induced Phase Shifting, *Jpn. J. Appl. Phys.*, 2005, **44**, 4548–4552.
- 29 N. Rapoport, *et al.*, Ultrasound-mediated tumor imaging and nanotherapy using drug loaded, block copolymer stabilized perfluorocarbon nanoemulsions, *J. Controlled Release*, 2011, **153**, 4–15.
- 30 Z. Z. Wong, O. D. Kripfgans, A. Qamar, J. B. Fowlkes and J. L. Bull, Bubble evolution in acoustic droplet vaporization at physiological temperature via ultra-high speed imaging, *Soft Matter*, 2011, **7**, 4009–4016.
- 31 T. J. Dubinsky, T. D. Khokhlova, V. Khokhlova and G. R. Schade, Histotripsy: The Next Generation of High-Intensity Focused Ultrasound for Focal Prostate Cancer Therapy, *J. Ultrasound Med.*, 2020, **39**, 1057–1067.
- 32 C. C. Chen, *et al.*, Targeted drug delivery with focused ultrasound-induced blood-brain barrier opening using acoustically-activated nanodroplets, *J. Controlled Release*, 2013, **172**, 795–804.
- 33 X. Song, L. Feng, C. Liang, K. Yang and Z. Liu, Ultrasound Triggered Tumor Oxygenation with Oxygen-Shuttle Nanoperfluorocarbon to Overcome Hypoxia-Associated Resistance in Cancer Therapies, *Nano Lett.*, 2016, **16**, 6145–6153.
- 34 W. Tang, *et al.*, Organic Semiconducting Photoacoustic Nanodroplets for Laser-Activatable Ultrasound Imaging and Combinational Cancer Therapy, *ACS Nano*, 2018, **12**, 2610–2622.
- 35 E. Vlasisavljevich, Y. Y. Durmaz, A. Maxwell, M. ElSayed and Z. Xu, Nanodroplet-mediated histotripsy for image-guided targeted ultrasound cell ablation, *Theranostics*, 2013, **3**, 851–864.

- 36 P. S. Sheeran and P. A. Dayton, Improving the Performance of Phase-Change Perfluorocarbon Droplets for Medical Ultrasonography: Current Progress, Challenges, and Prospects, *Scientifica*, 2014, **2014**, 1–24.
- 37 W. G. Pitt, R. N. Singh, K. X. Perez, G. A. Husseini and D. R. Jack, Phase transitions of perfluorocarbon nanoemulsion induced with ultrasound: A mathematical model, *Ultrason. Sonochem.*, 2014, **21**, 879–891.
- 38 T. Lacour, M. Guédra, T. Valier-Brasier and F. Coulouvrat, A model for acoustic vaporization dynamics of a bubble/droplet system encapsulated within a hyperelastic shell, *J. Acoust. Soc. Am.*, 2018, **143**, 23–37.
- 39 R. Melich, *et al.*, Microfluidic preparation of various perfluorocarbon nanodroplets: Characterization and determination of acoustic droplet vaporization (ADV) threshold, *Int. J. Pharm.*, 2020, **587**, 119651.
- 40 T. Giesecke and K. Hynynen, Ultrasound-mediated cavitation thresholds of liquid perfluorocarbon droplets in vitro, *Ultrasound Med. Biol.*, 2003, **29**, 1359–1365.
- 41 N. Chang, *et al.*, Efficient and controllable thermal ablation induced by short-pulsed HIFU sequence assisted with perfluorohexane nanodroplets, *Ultrason. Sonochem.*, 2018, **45**, 57–64.
- 42 M. L. Fabiilli, *et al.*, The role of inertial cavitation in acoustic droplet vaporization, *IEEE Trans. Ultrason. Ferroelectr. Freq. Control*, 2009, **56**, 1006–1017.
- 43 K. Wilson, K. Homan and S. Emelianov, Biomedical photoacoustics beyond thermal expansion using triggered nanodroplet vaporization for contrast-enhanced imaging, *Nat. Commun.*, 2012, **3**, 1–10.
- 44 K. Astafyeva, *et al.*, Perfluorocarbon nanodroplets stabilized by fluorinated surfactants: Characterization and potentiality as theranostic agents, *J. Mater. Chem. B*, 2015, **3**, 2892–2907.
- 45 R. Singh, G. A. Husseini and W. G. Pitt, Phase transitions of nanoemulsions using ultrasound: Experimental observations, *Ultrason. Sonochem.*, 2012, **19**, 1120–1125.
- 46 D. Pajek, A. Burgess, Y. Huang and K. Hynynen, High-Intensity Focused Ultrasound Sonothrombolysis: The Use of Perfluorocarbon Droplets to Achieve Clot Lysis at Reduced Acoustic Power, *Ultrasound Med. Biol.*, 2014, **40**, 2151–2161.
- 47 R. Williams, *et al.*, Characterization of Submicron Phase-change Perfluorocarbon Droplets for Extravascular Ultrasound Imaging of Cancer, *Ultrasound Med. Biol.*, 2013, **39**, 475–489.
- 48 T. Van Rooij, V. Daeichin, I. Skachkov, N. De Jong and K. Kooiman, Targeted ultrasound contrast agents for ultrasound molecular imaging and therapy, *Int. J. Hyperth.*, 2015, **31**, 90–106.
- 49 K. C. Schad and K. Hynynen, In vitro characterization of perfluorocarbon droplets for focused ultrasound therapy, *Phys. Med. Biol.*, 2010, **55**, 4933–4947.
- 50 P. S. Sheeran, *et al.*, Methods of generating submicrometer phase-shift perfluorocarbon droplets for applications in medical ultrasonography, *IEEE Trans. Ultrason. Ferroelectr. Freq. Control*, 2017, **64**, 252–263.
- 51 R. Chattaraj, G. M. Goldscheitter, A. Yildirim and A. P. Goodwin, Phase behavior of mixed lipid monolayers on perfluorocarbon nanoemulsions and its effect on acoustic contrast, *RSC Adv.*, 2016, **6**, 111318–111325.
- 52 P. A. Mountford, S. R. Sirsi and M. A. Borden, Condensation phase diagrams for lipid-coated perfluorobutane microbubbles, *Langmuir*, 2014, **30**, 6209–6218.
- 53 P. A. Mountford, A. N. Thomas and M. A. Borden, Thermal activation of superheated lipid-coated perfluorocarbon drops, *Langmuir*, 2015, **31**, 4627–4634.
- 54 S. K. Yarmoska, H. Yoon and S. Y. Emelianov, Lipid Shell Composition Plays a Critical Role in the Stable Size Reduction of Perfluorocarbon Nanodroplets, *Ultrasound Med. Biol.*, 2019, **45**, 1489–1499.
- 55 S. Schöttler, *et al.*, Protein adsorption is required for stealth effect of poly(ethylene glycol)- and poly(phosphoester)-coated nanocarriers, *Nat. Nanotechnol.*, 2016, **11**, 372–377.
- 56 N. Rapoport, *et al.*, Focused ultrasound-mediated drug delivery to pancreatic cancer in a mouse model, *J. Ther. Ultrasound*, 2013, **1**, 2–12.
- 57 P. Shende and S. Jain, Polymeric nanodroplets: an emerging trend in gaseous delivery system, *J. Drug Targeting*, 2019, **27**, 1035–1045.
- 58 C. Mannaris, *et al.*, Acoustically responsive polydopamine nanodroplets: A novel theranostic agent, *Ultrason. Sonochem.*, 2020, **60**, 104782.
- 59 D. Gao, *et al.*, Targeted ultrasound-triggered phase transition nanodroplets for Her2-overexpressing breast cancer diagnosis and gene transfection, *Mol. Pharm.*, 2017, **14**, 984–998.
- 60 Y. Cao, *et al.*, Drug release from phase-changeable nanodroplets triggered by low-intensity focused ultrasound, *Theranostics*, 2018, **8**, 1327–1339.
- 61 F. Baghbani, M. Chegeni, F. Moztarzadeh, S. Hadian-Ghazvini and M. Raz, Novel ultrasound-responsive chitosan/perfluorohexane nanodroplets for image-guided smart delivery of an anticancer agent: Curcumin, *Mater. Sci. Eng., C*, 2017, **74**, 186–193.
- 62 Z. Gao, A. M. Kennedy, D. A. Christensen and N. Y. Rapoport, Drug-loaded nano/microbubbles for combining ultrasonography and targeted chemotherapy, *Ultrasonics*, 2008, **48**, 260–270.
- 63 N. Y. Rapoport, A. M. Kennedy, J. E. Shea, C. L. Scaife and K. H. Nam, Controlled and targeted tumor chemotherapy by ultrasound-activated nanoemulsions/microbubbles, *J. Controlled Release*, 2009, **138**, 268–276.
- 64 M. Zhang, *et al.*, Initial Investigation of Acoustic Droplet Vaporization for Occlusion in Canine Kidney, *Ultrasound Med. Biol.*, 2010, **36**, 1691–1703.
- 65 E. Pisani, *et al.*, Perfluorooctyl bromide polymeric capsules as dual contrast agents for ultrasonography and magnetic resonance imaging, *Adv. Funct. Mater.*, 2008, **18**, 2963–2971.

- 66 K. Astafyeva, *et al.*, Properties of theranostic nanoparticles determined in suspension by ultrasonic spectroscopy, *Phys. Chem. Chem. Phys.*, 2015, **17**, 25483–25493.
- 67 N. Rapoport, Z. Gao and A. Kennedy, Multifunctional nanoparticles for combining ultrasonic tumor imaging and targeted chemotherapy, *J. Natl. Cancer Inst.*, 2007, **99**, 1095–1106.
- 68 G. Ji, J. Yang and J. Chen, Preparation of novel curcumin-loaded multifunctional nanodroplets for combining ultrasonic development and targeted chemotherapy, *Int. J. Pharm.*, 2014, **466**, 314–320.
- 69 C. Magnetto, *et al.*, Ultrasound-activated decafluoropentane-cored and chitosan-shelled nanodroplets for oxygen delivery to hypoxic cutaneous tissues, *RSC Adv.*, 2014, **4**, 38433–38441.
- 70 Q. Wei, *et al.*, Uniform-sized PLA nanoparticles: Preparation by premix membrane emulsification, *Int. J. Pharm.*, 2008, **359**, 294–297.
- 71 P. S. Sheeran, S. H. Luois, L. B. Mullin, T. O. Matsunaga and P. A. Dayton, Design of ultrasonically-activatable nanoparticles using low boiling point perfluorocarbons, *Biomaterials*, 2012, **33**, 3262–3269.
- 72 S. Ferri, *et al.*, Tailoring the size of ultrasound responsive lipid-shelled nanodroplets by varying production parameters and environmental conditions, *Ultrason. Sonochem.*, 2021, **73**, 105482.
- 73 O. D. Kripfgans, M. L. Fabiilli, P. L. Carson and J. B. Fowlkes, On the acoustic vaporization of micrometer-sized droplets, *J. Acoust. Soc. Am.*, 2004, **116**, 272–281.
- 74 T. O. Matsunaga, *et al.*, Phase-Change nanoparticles using highly volatile perfluorocarbons: Toward a platform for extravascular ultrasound imaging, *Theranostics*, 2012, **2**, 1185–1198.
- 75 N. Rapoport, *et al.*, Ultrasound-mediated tumor imaging and nanotherapy using drug loaded, block copolymer stabilized perfluorocarbon nanoemulsions, *J. Controlled Release*, 2011, **153**, 4–15.
- 76 A. L. Martin, *et al.*, Intracellular Growth of Nanoscale Perfluorocarbon Droplets for Enhanced Ultrasound-Induced Phase-Change Conversion, *Ultrasound Med. Biol.*, 2012, **38**, 1799–1810.
- 77 I. Gorelikov, A. L. Martin, M. Seo and N. Matsuura, Silica-coated quantum dots for optical evaluation of perfluorocarbon droplet interactions with cells, *Langmuir*, 2011, **27**, 15024–15033.
- 78 J. Y. Lee, *et al.*, Nanoparticle-Loaded Protein-Polymer Nanodroplets for Improved Stability and Conversion Efficiency in Ultrasound Imaging and Drug Delivery, *Adv. Mater.*, 2015, **27**, 5484–5492.
- 79 D. Meng, *et al.*, Charge-conversion and ultrasound-responsive O-carboxymethyl chitosan nanodroplets for controlled drug delivery, *Nanomedicine*, 2019, **14**, 2549–2565.
- 80 J. D. Rojas, M. A. Borden and P. A. Dayton, Effect of Hydrostatic Pressure, Boundary Constraints and Viscosity on the Vaporization Threshold of Low-Boiling-Point Phase-Change Contrast Agents, *Ultrasound Med. Biol.*, 2019, **45**, 968–979.
- 81 B. Helfield, *et al.*, Fluid Viscosity Affects the Fragmentation and Inertial Cavitation Threshold of Lipid-Encapsulated Microbubbles, *Ultrasound Med. Biol.*, 2016, **42**, 782–794.
- 82 A. A. Doinikov, P. S. Sheeran, A. Bouakaz and P. A. Dayton, Vaporization dynamics of volatile perfluorocarbon droplets: A theoretical model and in vitro validation, *Med. Phys.*, 2014, **41**, 1–10.
- 83 E. Vlaisavljevich, *et al.*, Effects of Droplet Composition on Nanodroplet-Mediated Histotripsy, *Ultrasound Med. Biol.*, 2016, **42**, 931–946.
- 84 D. S. Li, O. D. Kripfgans, M. L. Fabiilli, J. Brian Fowlkes and J. L. Bull, Initial nucleation site formation due to acoustic droplet vaporization, *Appl. Phys. Lett.*, 2014, **104**, 1–5.
- 85 C. J. Miles, C. R. Doering and O. D. Kripfgans, Nucleation pressure threshold in acoustic droplet vaporization, *J. Appl. Phys.*, 2016, **120**, 034903.
- 86 E. M. Strohm, I. Gorelikov, N. Matsuura and M. C. Kolios, Acoustic and photoacoustic characterization of micron-sized perfluorocarbon emulsions, *J. Biomed. Opt.*, 2012, **17**, 0960161.
- 87 G. M. Lanza, K. D. Wallace, M. J. Scott, W. P. Cacheris, D. R. Abendschein, D. H. Christy, A. M. Sharkey, J. G. Miller, P. J. Gaffney and S. A. Wickline, A novel site-targeted ultrasonic contrast agent with broad biomedical application, *Circulation*, 1996, **94**, 3334–3340.
- 88 P. S. Sheeran, *et al.*, Decafluorobutane as a Phase-Change Contrast Agent for Low-Energy Extravascular Ultrasonic Imaging, *Ultrasound Med. Biol.*, 2011, **37**, 1518–1530.
- 89 P. S. Sheeran, S. Luois, P. A. Dayton and T. O. Matsunaga, Formulation and acoustic studies of a new phase-shift agent for diagnostic and therapeutic ultrasound, *Langmuir*, 2011, **27**, 10412–10420.
- 90 O. Couture, *et al.*, Investigating perfluorohexane particles with high-frequency ultrasound, *Ultrasound Med. Biol.*, 2006, **32**, 73–82.
- 91 R. D. Airan, *et al.*, Noninvasive Targeted Transcranial Neuromodulation via Focused Ultrasound Gated Drug Release from Nanoemulsions, *Nano Lett.*, 2017, **17**, 652–659.
- 92 N. Reznik, *et al.*, The efficiency and stability of bubble formation by acoustic vaporization of submicron perfluorocarbon droplets, *Ultrasonics*, 2013, **53**, 1368–1376.
- 93 P. S. Sheeran, J. E. Streeter, L. B. Mullin, T. O. Matsunaga and P. A. Dayton, Toward Ultrasound Molecular Imaging With Phase-Change Contrast Agents: An In Vitro Proof of Principle, *Ultrasound Med. Biol.*, 2013, **39**, 893–902.
- 94 J. A. Feshitan, C. C. Chen, J. J. Kwan and M. A. Borden, Microbubble size isolation by differential centrifugation, *J. Colloid Interface Sci.*, 2009, **329**, 316–324.
- 95 P. Zhu and L. Wang, Passive and active droplet generation with microfluidics: a review, *Lab Chip*, 2017, **17**, 34–75.

- 96 G. F. Christopher and S. L. Anna, Microfluidic methods for generating continuous droplet streams, *J. Phys. D: Appl. Phys.*, 2007, **40**, R319.
- 97 F. Malloggi, *et al.*, Monodisperse colloids synthesized with nanofluidic technology, *Langmuir*, 2010, **26**, 2369–2373.
- 98 M. Seo, R. Williams and N. Matsuura, Size reduction of cosolvent-infused microbubbles to form acoustically responsive monodisperse perfluorocarbon nanodroplets, *Lab Chip*, 2015, **15**, 3581–3590.
- 99 N. Reznik, R. Williams and P. N. Burns, Investigation of vaporized submicron perfluorocarbon droplets as an ultrasound contrast agent, *Ultrasound Med. Biol.*, 2011, **37**, 1271–1279.
- 100 Y. Huang, *et al.*, Polymer-stabilized perfluorobutane nanodroplets for ultrasound imaging agents, *J. Am. Chem. Soc.*, 2017, **139**, 15–18.
- 101 X. Zhou, *et al.*, Ultrasound-responsive highly biocompatible nanodroplets loaded with doxorubicin for tumor imaging and treatment in vivo, *Drug Deliv.*, 2020, **27**, 469–481.
- 102 F. Yang, *et al.*, Superparamagnetic iron oxide nanoparticle-embedded encapsulated microbubbles as dual contrast agents of magnetic resonance and ultrasound imaging, *Biomaterials*, 2009, **30**, 3882–3890.
- 103 Z. Miao, *et al.*, Fabrication of a multimodal microbubble platform for magnetic resonance, ultrasound and fluorescence imaging application, *J. Nanosci. Nanotechnol.*, 2016, **16**, 2301–2306.
- 104 J. Jian, *et al.*, India ink incorporated multifunctional phase-transition nanodroplets for photoacoustic/ultrasound dual-modality imaging and photoacoustic effect based tumor therapy, *Theranostics*, 2014, **4**, 1026–1038.
- 105 A. S. Hannah, D. VanderLaan, Y.-S. Chen and S. Y. Emelianov, Photoacoustic and ultrasound imaging using dual contrast perfluorocarbon nanodroplets triggered by laser pulses at 1064 nm, *Biomed. Opt. Express*, 2014, **5**, 3042.
- 106 H. Yoon, Ultrasound and Photoacoustic Imaging of Laser-Activated Phase-Change Perfluorocarbon Nanodroplets, *Photonics*, 2021, **8**, 405.
- 107 H. Yoon, *et al.*, Contrast-enhanced ultrasound imaging in vivo with laser-activated nanodroplets, *Med. Phys.*, 2017, **44**, 3444–3449.
- 108 A. Hannah, G. Luke, K. Wilson, K. Homan and S. Emelianov, Indocyanine green-loaded photoacoustic nanodroplets: Dual contrast nanoconstructs for enhanced photoacoustic and ultrasound imaging, *ACS Nano*, 2014, **8**, 250–259.
- 109 D. Y. Santiesteban, D. S. Dumani, D. Profili and S. Y. Emelianov, Copper Sulfide Perfluorocarbon Nanodroplets as Clinically Relevant Photoacoustic/Ultrasound Imaging Agents, *Nano Lett.*, 2017, **17**, 5984–5989.
- 110 D. Y. Santiesteban, K. A. Hallam, S. K. Yarmoska and S. Y. Emelianov, Color-coded perfluorocarbon nanodroplets for multiplexed ultrasound and photoacoustic imaging, *Nano Res.*, 2019, **12**, 741–747.
- 111 X. Cheng, *et al.*, Ultrasound-triggered phase transition sensitive magnetic fluorescent nanodroplets as a multimodal imaging contrast agent in rat and mouse model, *PLoS One*, 2013, **8**, e85003.
- 112 C. H. Wang, S. T. Kang and C. K. Yeh, Superparamagnetic iron oxide and drug complex-embedded acoustic droplets for ultrasound targeted theranosis, *Biomaterials*, 2013, **34**, 1852–1861.
- 113 J. Liu, *et al.*, Low-intensity focused ultrasound (LIFU)-activated nanodroplets as a theranostic agent for noninvasive cancer molecular imaging and drug delivery, *Biomater. Sci.*, 2018, **6**, 2838–2849.
- 114 F. Maghsoudinia, *et al.*, Folic acid-functionalized gadolinium-loaded phase transition nanodroplets for dual-modal ultrasound/magnetic resonance imaging of hepatocellular carcinoma, *Talanta*, 2021, **228**, 122245.
- 115 A. M. Neubauer, S. D. Caruthers, F. D. Hockett, T. Cyrus, J. D. Robertson, J. S. Allen, T. D. Williams, R. W. Fuhrhop, G. M. Lanza and S. A. Wickline, Fluorine cardiovascular magnetic resonance angiography in vivo at 1.5 T with perfluorocarbon nanoparticle contrast agents, *J. Cardiovasc. Magn. Reson.*, 2007, **9**, 565–573.
- 116 M. M. Kaneda, S. Caruthers, G. M. Lanza and S. A. Wickline, Perfluorocarbon Nanoemulsions for quantitative molecular imaging and targeted therapeutics, *Ann. Biomed. Eng.*, 2009, **37**, 1922–1933.
- 117 S. D. Caruthers, T. Cyrus, P. M. Winter, A. Wickline and G. M. Lanza, Anti-angiogenic perfluorocarbon nanoparticles for diagnosis and treatment of atherosclerosis, *Wiley Interdiscip. Rev.: Nanomed. Nanobiotechnol.*, 2009, **1**, 311–323.
- 118 C. Crake, *et al.*, Combined passive acoustic mapping and magnetic resonance thermometry for monitoring phase-shift nanoemulsion enhanced focused ultrasound therapy, *Phys. Med. Biol.*, 2017, **62**, 6144–6163.
- 119 S. M. Janib, A. S. Moses and J. A. MacKay, Imaging and drug delivery using theranostic nanoparticles, *Adv. Drug Delivery Rev.*, 2010, **62**, 1052–1063.
- 120 M. L. Fabiilli, *et al.*, Assessment of the biodistribution of an [18F]FDG-loaded perfluorocarbon double emulsion using dynamic micro-PET in rats, *Contrast Media Mol. Imaging*, 2013, **8**, 366–374.
- 121 N. Amir, *et al.*, 18F-Labeled perfluorocarbon droplets for positron emission tomography imaging, *Nucl. Med. Biol.*, 2017, **54**, 27–33.
- 122 M. L. Hill, *et al.*, Towards a nanoscale mammographic contrast agent: Development of a modular pre-clinical dual optical/X-ray agent, *Phys. Med. Biol.*, 2013, **58**, 5215–5235.
- 123 M. Amrahli, *et al.*, Mr-labelled liposomes and focused ultrasound for spatiotemporally controlled drug release in triple negative breast cancers in mice, *Nanotheranostics*, 2021, **5**, 125–142.
- 124 V. Paefgen, D. Doleschel and F. Kiessling, Evolution of contrast agents for ultrasound imaging and ultrasound-mediated drug delivery, *Front. Pharmacol.*, 2015, **6**, 1–16.

- 125 N. Rapoport, A. M. Kennedy, J. E. Shea, C. L. Scaife and K. H. Nam, Ultrasonic nanotherapy of pancreatic cancer: Lessons from ultrasound imaging, *Mol. Pharm.*, 2010, **7**, 22–31.
- 126 E. Vlasisvljevich, *et al.*, Image-guided non-invasive ultrasound liver ablation using histotripsy: Feasibility study in an in vivo porcine model, *Ultrasound Med. Biol.*, 2013, **39**, 1398–1409.
- 127 F. Baghbani, M. Chegeni, F. Moztarzadeh, J. A. Mohandesi and M. Mokhtari-Dizaji, Ultrasonic nanotherapy of breast cancer using novel ultrasound-responsive alginate-shelled perfluorohexane nanodroplets: In vitro and in vivo evaluation, *Mater. Sci. Eng., C*, 2017, **77**, 698–707.
- 128 H. Zhao, *et al.*, Cell-penetrating peptide-modified targeted drug-loaded phase-transformation lipid nanoparticles combined with low-intensity focused ultrasound for precision theranostics against hepatocellular carcinoma, *Theranostics*, 2018, **8**, 1892–1910.
- 129 V. P. Torchilin, *et al.*, Cell transfection in vitro and in vivo with nontoxic TAT peptide-liposome-DNA complexes, *Proc. Natl. Acad. Sci. U. S. A.*, 2003, **100**, 1972–1977.
- 130 G. Mattheolabakis, L. Milane, A. Singh and M. M. Amiji, Hyaluronic acid targeting of CD44 for cancer therapy: From receptor biology to nanomedicine, *J. Drug Targeting*, 2015, **23**, 605–618.
- 131 L. Zhu, *et al.*, Peptide-Functionalized Phase-Transformation Nanoparticles for Low Intensity Focused Ultrasound-Assisted Tumor Imaging and Therapy, *Nano Lett.*, 2018, **18**, 1831–1841.
- 132 P. Tagde, G. T. Kulkarni, D. K. Mishra and P. Kesharwani, Recent advances in folic acid engineered nanocarriers for treatment of breast cancer, *J. Drug Delivery Sci. Technol.*, 2020, **56**, 101613.
- 133 W. Dong, *et al.*, Ultrasound-Mediated Gene Therapy of Hepatocellular Carcinoma Using Pre-microRNA Plasmid-Loaded Nanodroplets, *Ultrasound Med. Biol.*, 2020, **46**, 90–107.
- 134 W. Yang, H. Liang, S. Ma, D. Wang and J. Huang, Gold nanoparticle based photothermal therapy: Development and application for effective cancer treatment, *Sustainable Mater. Technol.*, 2019, **22**, e00109.
- 135 A. P. Castano, T. N. Demidova and M. R. Hamblin, Mechanisms in photodynamic therapy: Part one - Photosensitizers, photochemistry and cellular localization, *Photodiagn. Photodyn. Ther.*, 2004, **1**, 279–293.
- 136 R. A. Day and E. M. Sletten, Perfluorocarbon nanomaterials for photodynamic therapy, *Curr. Opin. Colloid Interface Sci.*, 2021, **54**, 101454.
- 137 J. Du, *et al.*, Enhanced photodynamic therapy for overcoming tumor hypoxia: From microenvironment regulation to photosensitizer innovation, *Coord. Chem. Rev.*, 2021, **427**, 213604.
- 138 W. W. Liu, *et al.*, Nanodroplet-Vaporization-Assisted Sonoporation for Highly Effective Delivery of Photothermal Treatment, *Sci. Rep.*, 2016, **6**, 1–14.
- 139 X. Tang, *et al.*, Overcome the limitation of hypoxia against photodynamic therapy to treat cancer cells by using perfluorocarbon nanodroplet for photosensitizer delivery, *Biochem. Biophys. Res. Commun.*, 2017, **487**, 483–487.
- 140 Y. Zhou, M. Wang and Z. Dai, The molecular design of and challenges relating to sensitizers for cancer sonodynamic therapy, *Mater. Chem. Front.*, 2020, **4**, 2223–2234.
- 141 X. Yi, *et al.*, IR-780 dye for near-infrared fluorescence imaging in prostate cancer, *Med. Sci. Monit.*, 2015, **21**, 511–517.
- 142 M. Svoboda, J. Riha, K. Wlcek, W. Jaeger and T. Thalhammer, Organic anion transporting polypeptides (OATPs): regulation of expression and function, *Curr. Drug Metab.*, 2011, **12**, 139–153.
- 143 S. M. Green, *et al.*, Role of OATP transporters in steroid uptake by prostate cancer cells in vivo, *Prostate Cancer Prostatic Dis.*, 2017, **20**, 20–27.
- 144 L. Zhang, *et al.*, Mitochondria-Targeted and Ultrasound-Activated Nanodroplets for Enhanced Deep-Penetration Sonodynamic Cancer Therapy, *ACS Appl. Mater. Interfaces*, 2019, **11**, 9355–9366.
- 145 Y. Zhang, L. Bi, Z. Hu, W. Cao and D. Zhuang, Hematoporphyrin monomethyl ether-mediated sonodynamic therapy induces A-253 cell apoptosis, *Oncol. Lett.*, 2020, **19**, 3223–3228.
- 146 C. Yang, *et al.*, Dual ultrasound-activatable nanodroplets for highly-penetrative and efficient ovarian cancer theranostics, *J. Mater. Chem. B*, 2020, **8**, 380–390.
- 147 L. Yao, *et al.*, Perfluorocarbon nanodroplets stabilized with cisplatin-prodrug-constructed lipids enable efficient tumor oxygenation and chemo-radiotherapy of cancer, *Nanoscale*, 2020, **12**, 14764–14774.
- 148 P. Prasad, *et al.*, Multifunctional Albumin À MnO<sub>2</sub> Nanoparticles Modulate Solid Tumor Microenvironment by Attenuating Enhance Radiation Response, *ACS Nano*, 2013, **8**, 3202–3212.
- 149 Y. J. Ho and C. K. Yeh, Concurrent anti-vascular therapy and chemotherapy in solid tumors using drug-loaded acoustic nanodroplet vaporization, *Acta Biomater.*, 2017, **49**, 472–485.
- 150 Y. Hu, *et al.*, Opto-acoustic synergistic irradiation for vaporization of natural melanin-cored nanodroplets at safe energy levels and efficient sono-chemo-photothermal cancer therapy, *Theranostics*, 2020, **10**, 10448–10465.
- 151 G. Song, *et al.*, TaOx decorated perfluorocarbon nanodroplets as oxygen reservoirs to overcome tumor hypoxia and enhance cancer radiotherapy, *Biomaterials*, 2017, **112**, 257–263.
- 152 D. S. Li, S. Schneewind, M. Bruce, Z. Khaing, M. O'Donnell and L. Pozzo, Spontaneous nucleation of stable perfluorocarbon emulsions for ultrasound contrast agents, *Nano Lett.*, 2018, **19**(1), 173–181.